PATENTS

IN THE UNITED STATES PATENT AND TRADEMARK OFFICE

Applicant(s):	Lieven De Veylder *et al.*	**Examiner:**	Cynthia Collins
Serial Number:	09/574,735	**Art Unit:**	1638
Filed:	May 18, 2000	**Docket:**	1187-2 CIP
For:	CYCLIN-DEPENDENT KINASE INHIBITORS AND USES THEREOF		

Commissioner for Patents
P.O. Box 1450
Alexandria, VA 22313-1450

DECLARATION PURSUANT TO 37 C.F.R. §1.132

Sir,

I, Catherine Bergounioux, declare as follows:

1. I am a French citizen residing at Gif sur Yvette, France.

2. I graduated from Clermont Fd University with a DEA degree in 1969 and from Paris Sud with a Doctor of Philosophy in 1978. From 1971 to 2005 I have held several positions at CNRS (Centre National de la Recherche Scientifique) and currently hold the position of Research Director at CNRS. I am first author or co-author of a number of scientific publications listed in my *curriculum vitae* (CV), attached herewith as Exhibit A.

3. Presently, I am Research Director of the Laboratoire Cycle Cellulaire, Institut de Biotechnologie des Plantes (Cell Cycle Laboratory, Institute of Plant Biotechnology), CNRS, Paris, France. In addition, I am Head of the "Activation and Inhibition of Cell Cycle During Plant Development Group" at this institution.

4. I have read the specification of the above-identified application and am familiar with the contents therein including the teaching of conserved sequence motifs within plant CKIs. In addition, I have reviewed presently pending claims 2, 5, 7-11, 14, 17, 21, 24, 25, 27, 30, 36-41, 43-45, 47-50, 52-57, as well as newly submitted claims 60-92.

5. I am co-author of an article published in the Journal of Cell Science 115(5), 973-982, 2002, provided herewith as Exhibit B.

6. The paper provided herewith at Exhibit B describes a CKI from tobacco, NtKIS1a, and the phenotypic characteristics of *Arabidopsis* plants transformed with the corresponding *NtKIS1a* gene under the control of the constitutive cauliflower mosaic virus 35S promoter. The transformed 35S::NtKIS1a plants showed reduced growth with smaller organs that contained larger cells; reduced CDK kinase activity, serrated leaves and reduced endoreduplication. These phenotypic characteristics are the same as those described in the above-identified application and as described in a publication by De Veylder *et al.*, The Plant Cell, Vol 13, 1653-1667, July 2001 (provided herewith as Exhibit C).

7. Although my co-authors and I used NtKIS1a in the paper provided at Exhibit B, it is my scientific belief that other CKI proteins could also be used to achieve the same results. The tobacco CKI, NtKIS1a, comprises a first sequence motif which is identical to the sequence set forth in the above-identified application as SEQ ID NO:34 as well as a second sequence motif comparable but not identical to the consensus sequence set forth in the above-identified application as SEQ ID NO:35 and a third sequence motif comparable but not identical to the consensus sequence set forth in the above-identified application as SEQ ID NO:36. Specifically, in NtKIS1a (NCBI Accession Number CAC82732), the sequence comparable to SEQ ID NO: 35 is: PSEGRYEW and the sequence comparable to SEQ ID NO: 36 is: EIEDFFAVRQ. The differences in the motifs of the tobacco sequences compared to the consensus sequences set forth in Table 2

(SEQ ID NOs: 35 and 36) of the above-identified application are underlined and boldfaced.

8. The consensus sequences of SEQ ID NO: 34, SEQ ID NO: 35 and SEQ ID NO: 36 (and also of consensus sequences SEQ ID NO: 37, SEQ ID NO: 38 and SEQ ID NO: 39) were also described in Table 1 of De Veylder *et al.* (see Exhibit C). Table 1 of De Veylder *et al.* is identical to Table 2 of the above-identified application except that Motif 1 of Table 1 is equivalent to Motif 2 or SEQ ID NO: 35 of Table 2 of the present application; and Motif 5 of Table 1 is equivalent to Motif 6 or SEQ ID NO: 39 of Table 2 of the present application. As taught on page 53 of the above-identified application, as well as column 1, page 1655 of the De Veylder publication provided at Exhibit C, the three domains located at the extremity of the C-terminal part of the proteins are shared by all CKIs (= KRPs) and are therefore important in identifying plant CKIs. It is my considered scientific opinion therefore, that one skilled in the art following the teachings of the above-identified application as of its filing date, as well as the literature extant at the time of filing, would have known that NtKIS1a was a CKI due to the presence of these three consensus sequences (SEQ ID NOs:34-36).

9. The consensus sequences shown in Table 2 of the present application vary somewhat from plant species to plant species. It is also my considered scientific opinion however, that one skilled in the art would recognize that even if the consensus sequences vary somewhat from plant to plant, a motif in a plant having about 70% identity (or one amino acid substitution) to the consensus sequences set forth in Table 2 (SEQ ID NOs:34-39), would be reasonably expected to function in the claimed invention with predictable results. Indeed, this is just what we have shown in our publication provided at Exhibit B with the results obtained from transformed 35S::NtKIS1a plants.

10. The foregoing paragraphs form the basis for my recognizing from the disclosure of the above-identified application, that Lieven DeVeylder et al., the applicants of the above-identified application, invented the presently claimed subject matter including the limitations recited therein, as of its filing date. The foregoing paragraphs

also form the basis for my belief that if I had had in hand both the disclosure of the above-identified application as well as the literature extant on the filing date of the above-identified application, I would have had every reasonable expectation of success in practicing the presently claimed invention. Thus, without having to engage in undue experimentation, one skilled in the art such as I would have had every reasonable expectation of success in practicing the presently claimed invention using a plant CKI comprising the consensus sequences set forth in SEQ ID NOs:34-36 and/or SEQ ID NOs:34-37 and/or SEQ ID NOs:34-39, including sequences having at least 70% identity thereto (or one amino acid substitution therein).

11. I declare under penalty of perjury under the laws of the United States of America that the foregoing is true and correct.

Dated _15 03 2005_____ _____
Catherine Bergounioux

BUNISSET Catherine épouse BERGOUNIOUX

Née le 6 mai 1946 à Davignac Corrèze France

11 bis chemin des Buttes
Gif sur Yvette
91190 France
Tel 0169073832

Directeur de Recherche au CNRS UMR8618
Institut de Biotechnologie des Plantes
Plateau de Moulon, Bât 630
Université Paris-Sud
91405 Orsay cedex France
Tel 33169153350
e.mail : Bergouni@ibp.u-psud.fr

Doctorat es-Sciences Naturelles : Université Paris-Sud ; 1978
Etude de l'intensité des manifestations de l'hétérosis au cours de l'ontogénèse du Pétunia hybrida

Directeur du laboratoire :
Activation et Inhibition du Cycle Cellulaire au Cours du Développement des plantes

Bibliographie

Raynaud C.,Cassier-Chauvat C.,Perennes C. and Bergounioux C. 2004 An arabidopsis homologue of the bacterial cell division inhibitor SulA is involved in plastid division. **Plant Cell** 16, 1801-11

Stevens R., Grelon M., Vezon D., Oh J., Meyer P., Domenichini S. and Bergounioux C. (2004) A R., *cdc45* homologue in *Arabidopsis thaliana* has a role in meiosis as shown by RNAi induced gene silencing. **Plant cell 16,** 99-113

Bertrand C, Bergounioux C, Domenichini S, Delarue M, Zhou DX. (2003). Arabidopsis histone acetyltransferase AtGCN5 regulates the floral meristem activity through the WUSCHEL/AGAMOUS Pathway. **J Biol Chem. 278(30),** 28246-51

Jasinski S, Saraiva L., Perennes C., Domenichini S., StevensR., Raynaud C. Bergounioux C. and Glab N. (2003) NtKIS2, a novel tobacco cyclin-dependent kinase inhibitor is differentially expressed during the cell cycle and plant development. **Plant Physiol. Bioch** 41 (3), 503-676.

Jasinski S. Perennes C., Bergounioux C. and Glab N. (2002) Comparative molecular and functional analyses of the tobacco CDK inhibitor NtKIS1a and its spliced variant NtKIS1b. **Plant Physiol 130(4):**1871-82.

Jasinski S., Riou-Kamlichi C., Perennes C., Bergounioux C. and Glab N.(2002) The CDK inhibitor NtKIS1a is involved in plant development,endoreduplication and restores normal development of cyclinD3;1overexpressing plants. **J. Cell Sci., 115,** 973-982.

Mariconti L., Pellegrini B., Cantoni R., Steven,s R. Bergounioux C. Cella R.and Albani D (2002).The E2F family of transcription factors from *Arabidopsis thaliana*: Novel and conserved components of the RB/E2F pathwayin plants. **J. Biol. Chem., 277,** 9911-9919.

Rossignol P., Stevens R., Perennes C., Jasinski S., Cella R., Tremoussaygue D. and Bergounioux C. (2002) At E2F-a and AtDP-a, members of the E2F familyof transcription factors, induce *Arabidopsis* leaf cells to re-enter Sphase. **Mol. Genet. Genomics, 266,** 995- 1003.

Stevens R., Mariconti L., Rossignol P., Perennes C., Cella R., Bergounioux C. (2002) Two E2F Sites in the *Arabidopsis* MCM3 Promoter Have Different Roles in Cell Cycle Activation and Meristematic Expression. **J. Biol. Chem.,277,**32978-84.

Planchais S., Perennes C., Glab N., Mironov V., Inze D., Bergounioux C. (2002) Characterization of cis-acting element involved in cell cycle phase-independent activation of Arath;CycB1;1 transcription and identification of putative regulatory proteins. **Plant Mol. Biol.,50,**111-27.

The CDK inhibitor NtKIS1a is involved in plant development, endoreduplication and restores normal development of cyclin D3;1-overexpressing plants

Sophie Jasinski[1,‡], Catherine Riou-Khamlichi[2,*], Odile Roche[3], Claudette Perennes[1], Catherine Bergounioux[1] and Nathalie Glab[1]

[1]Laboratoire Cycle Cellulaire, Institut de Biotechnologie des Plantes, CNRS UMR8618, Université Paris-Sud, 91405 Orsay Cedex, France
[2]Institute of Biotechnology, University of Cambridge, Tennis Court Road, Cambridge, CB2 1QT, UK
[3]Service de Cytologie, Institut de Biotechnologie des Plantes, CNRS UMR8618, Université Paris-Sud, 91405 Orsay Cedex, France
*Present address: Institut des Sciences de la Vie et de la Santé, EA 3176, Université de Limoges, 87060 Limoges Cedex, France
‡Author for correspondence (e-mail: jasinski@ibp.u-psud.fr)

Accepted 3 December 2001
Journal of Cell Science 115, 973-982 (2002)

Summary

Plant development requires stringent controls between cell proliferation and cell differentiation. Proliferation is positively regulated by cyclin dependent kinases (CDKs). Acting in opposition to CDKs are CDK inhibitors (CKIs). The first tobacco CKI (NtKIS1a) identified was shown to inhibit in vitro the kinase activity of CDK/cyclin complexes and to interact with CDK and D-cyclins. However, these features, which are common to other plant and animal CKIs already characterised, did not provide information about the function of NtKIS1a in plants. Thus, to gain insight into the role of NtKIS1a and especially its involvement in cell proliferation during plant development, we generated transgenic *Arabidopsis thaliana* plants that overexpress *NtKIS1a*. These plants showed reduced growth with smaller organs that contained larger cells. Moreover, these plants displayed modifications in plant morphology. These results demonstrated that plant organ size and shape, as well as organ cell number and cell size, might be controlled by modulation of the single *NtKIS1a* gene activity. Since in mammals, D-cyclins control cell cycle progression in a CDK-dependent manner but also play a CDK independent role by sequestering the CKIs $p27^{Kip1}$ and $p21^{Cip1}$, we tested the significance of cyclin D-CKI interaction within a living plant. With this aim, *NtKIS1a* and *AtCycD3;1* were overexpressed simultaneously in plants by two different methods. Our results demonstrated that overexpression of the CKI *NtKIS1a* restores essentially normal development in plants overexpressing *AtCycD3;1*, providing the first evidence of cyclin D-CKI co-operation within the context of a living plant.

Key words: *Arabidopsis thaliana*, CDK inhibitor, Cyclin D, Endoreduplication, Plant development

Introduction

Developmental control of morphogenesis requires the co-ordination between cell proliferation, cell growth and cell differentiation. Because plant cells do not move and are surrounded by a rigid cell wall, a co-ordinated control of cell division is likely to be important in both environmental responses and developmental processes. Nonetheless, the mechanisms that link developmental events to the cell cycle machinery that controls cell proliferation remain poorly understood. Cell proliferation is precisely controlled by growth stimulatory and inhibitory signals transduced from the extracellular environment (Trehin et al., 1998). Cell cycle regulators such as CDKs, cyclins or CDK inhibitors integrate these signals. For example, D-cyclins are modulated by plant growth regulators and sucrose, and are thought to be important for stimulatory growth signal transduction between the environment and the cell cycle machinery (Meijer and Murray, 2000; Stals and Inze, 2001). Furthermore, expression of the CDK inhibitor *ICK1* is induced by abscisic acid, another growth regulator that prevents cell division (Wang et al., 1998).

In vertebrates, the existence of pathways linking development to cell cycle control was revealed by the occurrence of developmental defects that result from targeted mutation or overexpression of genes involved in cell cycle function, such as cyclin D or the retinoblastoma family (Cobrinik et al., 1996; Sicinski et al., 1995).

Because some of the inhibitory signals are believed to be mediated by CDK inhibitors, it is possible that these molecules contribute to cell cycle exit during differentiation. Consistent with this hypothesis, in double mutant mice lacking both functional $p27^{Kip1}$ and $p57^{Kip2}$, or $p21^{Cip1}$ and $p57^{Kip2}$ CDK inhibitors, numerous cell types fail to differentiate during embryonic development (Zhang et al., 1998; Zhang et al., 1999). CDK inhibitors may also play a direct role in stimulating differentiation (Ohnuma et al., 1999). Although the signals that activate CKIs during differentiation remain unknown, these CKIs clearly provide a crucial link between cell-cycle arrest and differentiation (Myster and Duronio, 2000). In plants, activation of division by overexpressing *AtCycD3;1* or inhibition of division by overexpressing *ICK1* or *KRP2* induced profound effects on plant growth and development, providing a link between cell cycle regulation and development (De Veylder et al., 2001; Riou-Khamlichi et al., 1999; Wang et al., 2000).

Using a two-hybrid approach, we recently characterised the first tobacco CKI named *NtKIS1a*. Its deduced polypeptide sequence displayed strong similarity with plant CKIs and with the mammalian CDK inhibitor CIP/KIP family (S.J., C.B. and N.G., unpublished). The similarity between these proteins consists of a highly conserved domain similar to the CDK interaction/inhibition domain identified in the animal CIP/KIP inhibitors (Chen et al., 1996; Russo et al., 1996). Consistent with this, we showed that NtKIS1a inhibited the kinase activity of BY-2 cell CDK/cyclin complexes. In a two-hybrid system, NtKIS1a interacted with both CDK and D-cyclins but not with PCNA, suggesting that it was more closely related to $p27^{Kip1}$ than to $p21^{Cip1}$ (S.J., C.B. and N.G., unpublished).

In mammals, recent work indicates that the induction of cyclin D-CDK complexes results in a redistribution of CDK inhibitors $p27^{Kip1}$ and $p21^{Cip1}$ from cyclin E-CDK2 complexes to cyclin D-CDK4/6 complexes, thereby triggering the kinase activity of cyclin E-CDK2 (Sherr and Roberts, 1999). Thus, mammalian D-cyclins also control cell cycle progression in a kinase independent manner, via interaction with CIP/KIP.

In this study, we examined the effects of *NtKIS1a* overexpression on plant development. Gain of NtKIS1a function decreased organ size and increased cell size. Furthermore, it blocked the endoreduplication phenomenon. The significance of cyclin D-CKI interaction within the context of a living *Arabidopsis* was studied. With this aim, we took advantage of *AtCycD3;1*-overexpressing plants (Riou-Khamlichi et al., 1999), which had leaves curled along their proximal-distal axis and contained numerous small and incompletely differentiated cells (Meijer and Murray, 2001). We generated plants that overexpressed both *AtCycD3;1* and *NtKIS1a*. Analysis of these plants provided evidence for AtCycD3;1 and NtKIS1a interaction in planta.

Materials and Methods

Transgene constructs and *Arabidopsis thaliana* transformation

The full length cDNAs encoding *NtKIS1a* or *NtKIS1b* were cloned into pCW162. These plasmids were introduced into *Agrobacterium tumefaciens* (HBA10S). *Arabidopsis thaliana* plants, ecotype 'Columbia', were transformed with these constructions as previously described (Bechtold and Pelletier, 1998). Seeds from the *Agrobacterium*-treated plants were selected on 0.5× Murashige and Skoog medium containing 50 mg/l kanamycin (MS-Km). Kanamycin-resistant (Km^R) plantlets (T1) were transferred to soil in the greenhouse under long-day conditions (16 hours light) and the presence of the *NtKIS1a* or *NtKIS1b* cDNA was controlled by PCR. A study of the phenotype was carried out and the seeds were collected and plated onto MS-Km. 12 Km^R T2 plantlets from 20 T1 lines were transferred to the greenhouse and throughout their phenotype analysis we focused on four lines.

Transformation of *A. thaliana AtCycD3;1*-overexpressing plants was similarly performed, except that the *NtKIS1a* cDNA was cloned into Bin-Hyg-TX vector. Seeds from the *Agrobacterium*-treated plants were selected on MS-Km containing 25 mg/l hygromycin.

Genomic DNA extraction for PCR

Leaf fragments were ground in an extraction buffer (200 mM Tris-HCl, pH 7.5, 250 mM NaCl, 25 mM EDTA, 0.5% SDS). PCR, using the Promega TfiI DNA polymerase, was performed in the presence of 2% DMSO on DNA from the isopropanol-precipitated supernatant.

RNA isolation and RT-PCR analysis

A. thaliana cauline leaves were frozen and ground in a mortar to perform total RNA extraction using TRIzol reagent (Life Technologies). For RT-PCR analysis, first-strand cDNA was synthesised from 5 μg of total RNA using SuperscriptII RNase H-Reverse Transcriptase (Life Technologies) following the manufacturer's instructions. 2.5 μl were used for PCR in a final volume of 25 μl. PCR products were then analysed on a 1% agarose gel and transferred onto a Hybond N+ membrane (Amersham). Hybridisations were performed at 62°C according to Church and Gilbert's protocol (Church and Gilbert, 1984). *NtKIS1a*, *AtCycD3;1* and *Actin2* probes correspond to the coding sequences.

Analyses by light and SEM microscopy

WT and 35S::NtKIS1a flowers were fixed with FAA (50% EtOH, 5% acetic acid, 10% formaldehyde), dehydrated in increasing ethanol concentrations and in propylene oxide and embedded in araldite resin for 60 hours at 48°C. 1.5 μm sections were cut with an LKB ultrotome III ultramicrotome, coloured with 0.5% toluidine blue and observed under a light microscope.

WT and 35S::NtKIS1a leaves of 1 cm were analysed with a scanning electron microscope (Hitachi S-3000N) under the ESED mode. Samples were slowly frozen at −12°C under partial vacuum on the Peltier stage before observation. Cell area was measured using the Optimas 6.0 software.

Flow cytometric analyses

Leaf fragments from WT, 35S::NtKIS1a and 35S::NtKIS1b plants were chopped in Galbraith's buffer (Galbraith et al., 1983). Mixtures were filtered and released nuclei were stained with Dapi and analysed using a flow cytometer (Vantage, Coulter).

Histone H1 kinase assay

$p9^{CKSHs1}$ beads were prepared as described (Azzi et al., 1992). *A. thaliana* plantlets (approximately 500 mg of fresh material) were ground in a mortar in liquid nitrogen with 1 ml of extraction buffer (25 mM MOPS pH 7.2, 60 mM β-glycerophosphate, 15 mM p-nitrophenylphosphate, 15 mM EGTA, 15 mM $MgCl_2$, 1 mM DTT, 1 mM NaF, 1 mM NH_4VO_3, 1 mM phenylphosphate, 0.2 μg/ml leupeptin, 0.3 μg/ml pepstatin). The resulting powder was slowly thawed on ice and centrifuged for 30 minutes at 18,000 *g* at 4°C to eliminate cell debris. Protein extract (570 μg) was added to 10 μl of packed $p9^{CKSHs1}$ beads previously washed three times with bead buffer (Azzi et al., 1992) and kept under rotation at 4°C for 1 hour 30 minutes. After a centrifugation pulse and removal of the supernatant, beads were washed three times with bead buffer and used for H1K assays. Samples containing the initial 10 μl packed beads were incubated for 30 minutes at 30°C with 1 μCi[γ-^{32}P]ATP, 25 μg histone H1 (Sigma) in a final volume of 30 μl H1K assay buffer (Azzi et al., 1992). The reaction was stopped by placing samples on ice. After a centrifugation pulse, Laemmli buffer was added to 15 μl of supernatant. Samples were analysed by 12% SDS-PAGE followed by Coomassie blue staining to visualise histone H1 and autoradiography to detect histone H1 phosphorylation, which was further quantified with the NIH image 1.62 software.

Western blotting

After H1K assays, proteins bound to $p9^{CKSHs1}$ beads were recovered by boiling in the presence of Laemmli buffer, run on 12% SDS-PAGE gels and transferred to a 0.1 μm nitrocellulose membrane for 1 hour in a semi-dry system (Millipore) at 2.5 V/cm^2. The membrane was further treated as described in the ECL+Plus System protocol (Amersham). The primary antibody was a monoclonal anti-PSTAIR

antibody (Sigma), and the secondary one was a goat anti-mouse peroxidase conjugated antibody (BioRad). Detection of the target proteins was performed by chemoluminescence using the ECL+Plus System (Amersham).

Yeast two-hybrid assays

Yeast two-hybrid assays were performed according to the protocol described in the Matchmaker Two-Hybrid system (Clontech).

Results

The overexpression of the CDK inhibitor NtKIS1a induces serrated leaves and abnormal flowers

To examine the roles of NtKIS1a on plant growth and development, *A. thaliana* transgenic lines in which the *NtKIS1a* cDNA was expressed under the control of the constitutive cauliflower mosaic virus 35S promoter were generated. *NtKIS1b* cDNA, a spliced variant expressed in planta, was used as control. NtKIS1b did not interact with A-type CDK nor with D-type cyclins and did not inhibit the kinase activity of CDK/cyclin complexes (S.J., C.B. and N.B., unpublished). The presence of the *NtKIS1a* or *NtKIS1b* cDNAs was controlled on genomic DNA in the Kanamycin-resistant (Km^R) T1 plantlets and their effective expression was monitored using RT-PCR analyses. The 35S::NtKIS1b T1 plants displayed no significant difference compared with WT plants (Fig. 1A,d,e). By contrast, 40% (16 from 40 independent lines) of 35S::NtKIS1a T1 plants showed phenotypic modifications. Serrated and/or undulated leaves were observed in all the 16 plants. However, we noticed a gradient in the undulation, the depth and the number of the teeth with deeper and more numerous teeth in the strongest phenotype. Fig. 1Aa,b,c represented rosette leaves, referred to as weak, medium and strong phenotypes, respectively. Not only was the leaf margin affected, but also the rosette diameter was reduced, as measured in the next generations (Fig. 1B). Compared with wildtype (WT), the flowering time was advanced in several lines (not shown). Furthermore, in five lines that harboured the strong leaf phenotype (Fig. 1A,c), flowers were smaller and did not give seeds (Fig. 1A,f,g). The phenotype of these lines, which were lost, was referred to as 'extreme' in the text.

The T2 progeny of four T1 lines (one displaying a strong, one displaying a medium, and two displaying no significant or a weak phenotype) was analysed. According to the number of T2 plants displaying a serrated leaf phenotype, three cases were observed. In the first case, which described the progeny of a T1 strong line, 12 plants out of 12 grown, presented the serrated phenotype with a gradient in the depth of the teeth. Among these 12 plants, 5 displayed a more severe phenotype than the T1 parents, were affected in flower morphology and were sterile. In the second case, which described the progeny of a T1 medium line, 8 plants out of 12 were affected in leaf morphology but remained fertile. Finally, in the third case, which described the progeny of a weak T1 line, only 1 plant out of 12 T2 presented serrated leaves and was fertile (Fig. 1C). The number of T2 plants that displayed a serrated phenotype was assumed to reflect the disjunction of the transgene insertions present in the T1 parents. Interestingly, we observed stronger phenotypes when there were more T2 plants affected (Fig. 1C). Consequently, it was suggested that the strength of

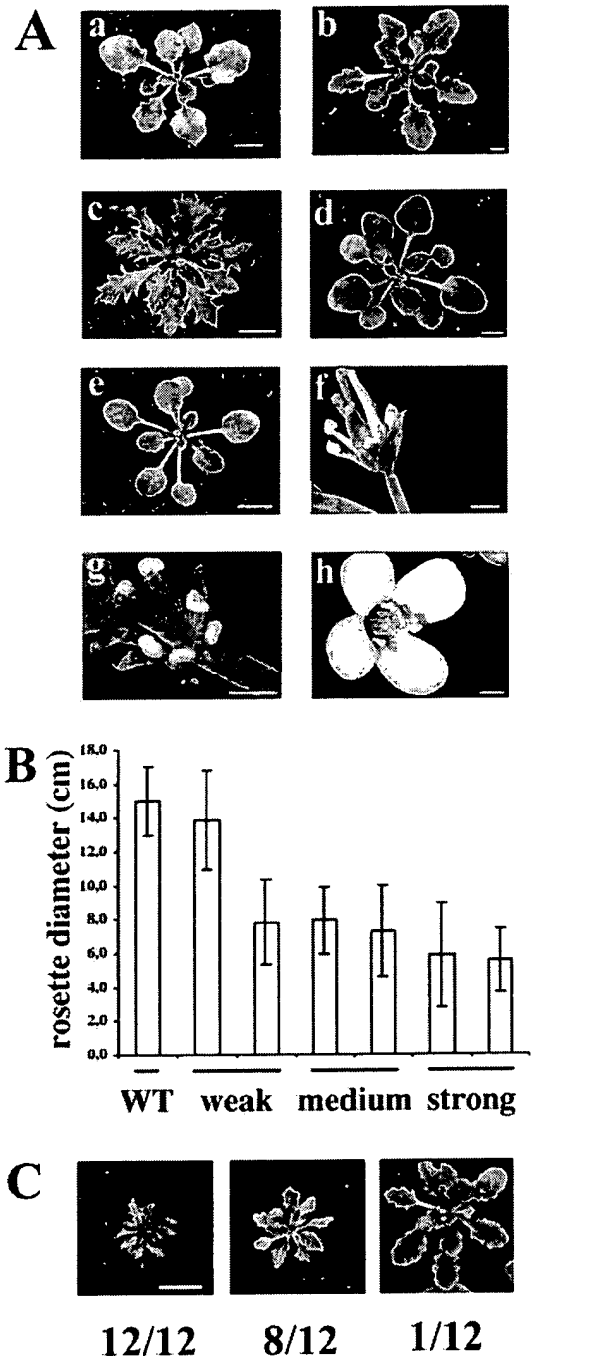

Fig. 1. Gain of function of NtKIS1a produces serrated leaves, abnormal flowers and reduces plant size. (A) Rosettes from three T1 35S::NtKIS1a independent lines, displaying respectively a weak (a), medium (b) and strong (c) serrated leaf phenotype, are compared with 35S::NtKIS1b (d) or WT (e) rosette. Abnormal flowers from 35S::NtKIS1a line displaying an extreme phenotype (f,g; see text) are compared with WT flower (h). Bars, 5 mm (a-e); 0.5 mm(f-h). (B) The rosette diameter of 24 plants (5-week-old) from 2 weak, 2 medium and 2 strong lines were measured. The graph represents the average diameter ± s.d. (C) Three cases were met according to the number of T2 plants displaying a serrated leaf phenotype in 12 Km^R plants analysed. For each case, a serrated plant is shown. Bar, 10 mm.

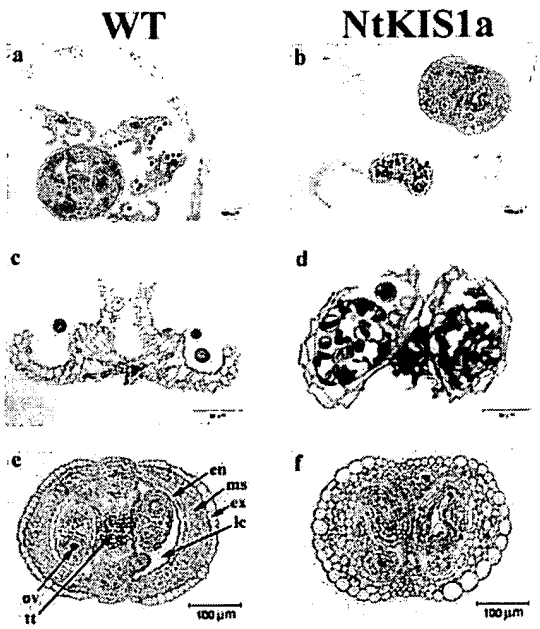

Fig. 2. *NtKIS1a* overexpression induces anther and gynoecium disorganised structure. Transverse sections of flowers from wildtype (WT) or a 35S::NtKIS1a line displaying an extreme phenotype (NtKIS1a) were performed. a and b corresponded to general views. More detailed views of anthers (c,d) and ovaries (e,f) are shown. In WT ovary, exocarp (ex), mesocarp (ms), and endocarp (en) layers could be distinguished. The dark staining cells of the transmitting tract (tt) occupied the inner portion of the ovary. Inside the locules (lc), ovules (ov) were visible in WT and NtKIS1a.

the phenotype was to some extent related to the number of transgene insertions.

Closer inspection of the extreme flower phenotype showed a conservation of all the whorls with, however, a reduced growth of petals and stamens (Fig. 1A,f,g). To understand the reasons for the sterility, flower transversal sections of WT and 35S::NtKIS1a were compared (Fig. 2). In 35S::NtKIS1a anthers, pollen grains were formed. Nevertheless, they showed a strong heterogeneity in size. Furthermore, the anthers had a disorganised structure and failed to dehisce (Fig. 2b,d). The gynoecium structure was also affected (Fig. 2f). Its organisation in three layers, exo, meso and endocarp, was not clearly observed compared with the WT (Fig. 2e). Moreover, most of the cells were enlarged and their shape seemed to be modified. Additionally, the transmitting tract, a tissue specialised in directing pollen tube growth, was nearly absent in 35S::NtKIS1a. The ovules displayed a disorganised structure but were apparently not affected in number.

35S::NtKIS1a plants show reduced CDK kinase activity

The CDK kinase activity was analysed in two 35S::NtKIS1a lines, one strong and one medium. Results shown in Fig. 3 demonstrated that the CDK kinase activity measured in these lines was significantly decreased compared with WT. Moreover, since 60% inhibition was observed in strong line and 37% in the medium one, it suggested that the CDK kinase activity inhibition was correlated to the strength of the phenotype.

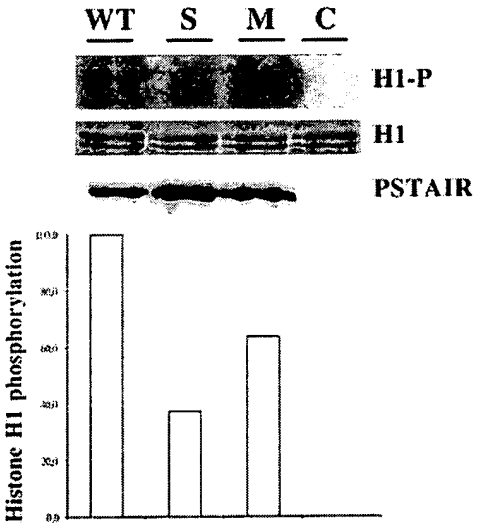

Fig. 3. The CDK kinase activity of 35S::NtKIS1a lines is reduced. Protein extracts from wildtype (WT), two 35S::NtKIS1a *Arabidopsis* lines, one strong (S) and one medium (M), or buffer (C) were added to $p9^{CKSHs1}$ beads to purify CDK/cyclin complexes. Histone H1 phosphorylation (H1-P) was monitored and equal loading of histone H1 (H1) was controlled. Proteins bound to $p9^{CKSHs1}$ beads were recovered and immunoblotted with an antibody raised against the conserved CDK PSTAIR motif (PSTAIR). The histone H1 phosphorylation and the PSTAIR signals were quantified with NIH image 1.62 software. Their ratio was calculated and presented in the graph. The maximal value obtained in WT was referred as 100%.

Gain of NtKIS1a function in *Arabidopsis* plants decreases organ size and increases cell size

The decrease in plant and organ size observed in the 35S::NtKIS1a lines could reflect an alteration in cell size and/or cell number. To investigate this last point at the cellular level, we examined the size of cells in 35S::NtKIS1a petals and leaves in comparison with the wildtype (Fig. 4). In WT petals, the shape and size of the cells were different along the organ and defined three regions: basal (III), median (II) and distal (I) (Fig. 4A,B). In the basal and median regions, the cells had a lengthened shape, basal cells being larger than median cells, whereas in the distal region, cells had a round shape and a small size. Interestingly, in the 35S::NtKIS1a, the cells had a constant lengthened shape all along the petal. The distal cells were still smaller than the basal cells but had lost their round shape. Moreover, the petal margin was serrated (Fig. 4B). Comparison of cells from WT and 35S::NtKIS1a demonstrated that the cell size at all three regions was significantly increased in the outer epidermis of 35S::NtKIS1a petals (Fig. 4C). Since 35S::NtKIS1a petals were smaller, it suggested that petals had fewer cells per organ than the WT.

The size of leaf lower epidermis cells from two 35S::NtKIS1a lines was analysed using scanning electron microscopy and the cell area was further quantified using the optimas 6.0 software. The results show that the cells were significantly enlarged in *NtKIS1a*-overexpressing plants compared with a WT plant (Fig. 4D). In WT, cell area varied from 180 to 3516 μm^2 and three categories of

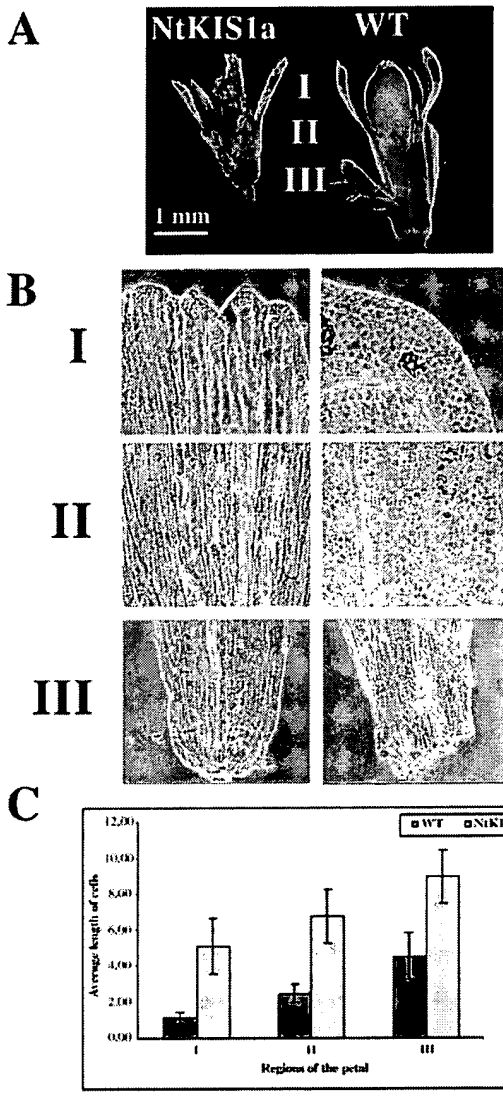

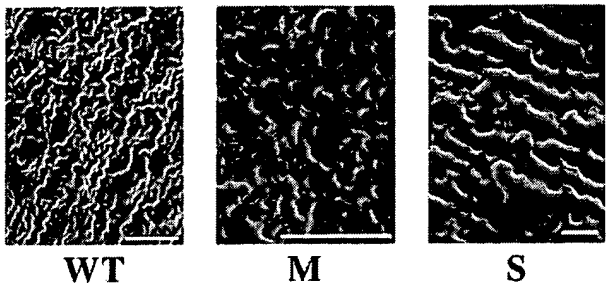

E

	area		
	< 300	300 - 3 000	>3 000
WT	230 (n=8)	1 026 (n=48)	3 242 (n=8)
NtKIS1a (line M)	n.o.	2 041 (n=18)	4 392 (n=17)
NtKIS1a (line S)	n.o.	n.o.	20 369 (n=21)

Fig. 4. Overexpression of *NtKIS1a* decreases organ size in increasing cell size. (A) A photograph of flowers from an extreme 35S::NtKIS1a line (NtKIS1a) and from wildtype (WT) indicating the three regions (I, II, III) of the petal that were used for microscopic analysis. (B) Light microscopic analysis of outer epidermal cells at three positions (I, II and III) of 35S::NtKIS1a and WT petal. (C) Cell size in the three regions of 35S::NtKIS1a and WT petals. Bars indicate s.d. (D) Scanning electron microscopy of the leaf lower epidermis of WT and two 35S::NtKIS1a *Arabidopsis* lines, one medium (M) and one strong (S). Bars, 100 μm. (E) From several scanning electron microscopy images of the lines described in D, cell areas were measured using the Optimas 6.0 software. The mean cell areas were reported in three categories: areas less than 300 μm^2, areas between 300 and 3000 μm^2 and areas greater than 3000 μm^2 (n.o. correspond to categories not observed). The number of cells (n) recorded in each categories is indicated in brackets.

cell area can be described: area less than 300 μm^2; area between 300 and 3000 μm^2; and area greater than 3000 μm^2 (Fig. 4E). In the 35S::NtKIS1a line displaying a medium phenotype, cells with an area less than 300 μm^2 were never observed. Additionally, in the two remaining groups, the average cell area was increased. In the 35S::NtKIS1a line displaying a strong phenotype, only cells with an area greater than 3000 μm^2 were observed, on average 6.3-fold higher than the corresponding cell area in the WT (Fig. 4E).

Rosette leaves of 35S::NtKIS1a plants display a decreased DNA content

Most *Arabidopsis* organs consist of cells with polyploid nuclei attributable to endoreduplication, which increases cell size (Bergounioux et al., 1992; Koornneef, 1994). Since an increase in size was revealed in 35S::NtKIS1a plant cells, the ploidy level in different organs of 35S::NtKIS1a, 35S::NtKIS1b and WT plants was compared by flow cytometric analysis. In rosette leaf cells of WT plants, the maximal endoreduplication level reached 64C, the proportion of cells with a high DNA content increased with leaf aging, as already observed (S.C. Brown, personal communication). Conversely, the distribution pattern of DNA content in cauline leaves was modified and reached a 2C and 4C distribution in flower buds. Surprisingly, in 35S::NtKIS1a plants displaying a strong phenotype, cells of all the tested organs, even the rosette leaves, displayed a 2C and 4C DNA content distribution (Fig. 5). This result demonstrated that the endoreduplication phenomenon was absent in these 35S::NtKIS1a plants. Moreover, in these plants, the proportion of 4C DNA content cells was very low resulting in an overwhelming 2C DNA content cell population.

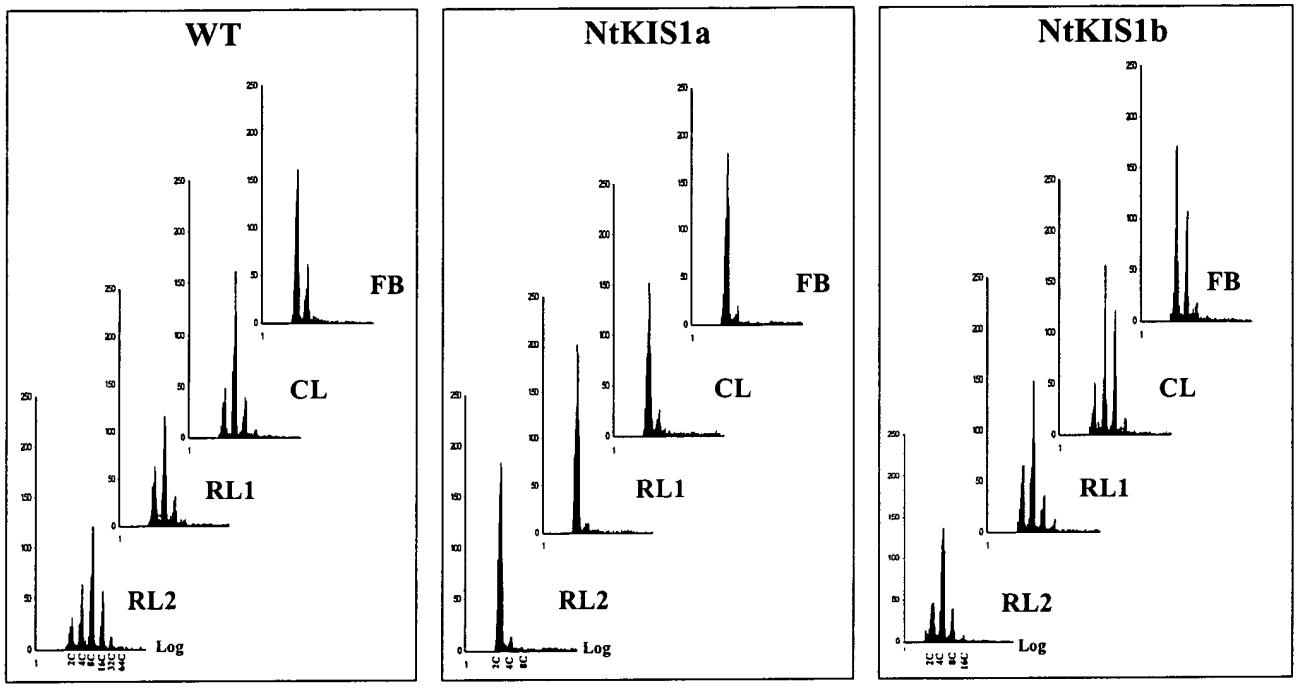

Fig. 5. Overexpression of *NtKIS1a* inhibits rosette leaf cell endoreduplication. Ploidy distributions for nuclei isolated from old (RL2) and young (RL1) rosette leaves, cauline leaves (CL) and flower buds (FB) of *A. thaliana* wildtype (WT), strong 35S::NtKIS1a (NtKIS1a) or 35S::NtKIS1b (NtKIS1b) lines. For each sample, 5000 DAPI-stained nuclei were analysed. The *x*-axis represents DNA fluorescence in logarithmic scale and DNA content is indicated. The *y*-axis represents frequency.

Overexpression of *NtKIS1a* rescues normal development in *AtCycD3;1*-overexpressing plants

The flow cytometric analysis performed on *NtKIS1a*-overexpressing *Arabidopsis* plants suggested that NtKIS1a prevents endoreduplication and may influence S phase progression. Therefore, to gain more insight into the various pathways in which NtKIS1a could be involved we first hypothesised that it might interact with D-cyclin/CDK complexes. Indeed, we previously showed that NtKIS1a interacts with tobacco D-cyclins in a yeast two-hybrid system (S.J., C.B. and N.G., unpublished). Additionally, the *Arabidopsis* D-cyclin AtCycD3;1 represented one of the preys obtained in a two-hybrid screen using NtKIS1a as a bait (S.J., C.B. and N.G., unpublished). This interaction was further confirmed (Fig. 6A), demonstrating that these two proteins were interacting partners in a two-hybrid system. In *Arabidopsis*, *AtCycD3;1* overexpression resulted in the formation of abnormal plants that contained numerous small, incompletely differentiated cells (Meijer and Murray, 2001). Moreover, these plants showed disorganised meristem, late flowering and delayed senescence (Riou-Khamlichi et al., 1999).

To determine whether NtKIS1a could inhibit the CDK/cyclin D3;1 activity and thus rescue the *AtCycD3;1*-overexpression phenotype, NtKIS1a and AtCycD3;1 were combined in the context of a living *Arabidopsis* plant by two different methods. First, we performed hand-pollination of *AtCycD3;1* pistils with *NtKIS1a*-overexpressing pollen. The presence of both *AtCycD3;1* and *NtKIS1a* transgenes was controlled in F1 plants by PCR analysis (not shown) and their effective overexpression was checked by RT-PCR (Fig. 6B, left). Interestingly, the phenotype of the AtCycD3;1×NtKIS1a plants was similar to that of the WT, making clear differences to those observed in both *AtCycD3;1* or *NtKIS1a*-overexpressing plants (Fig. 6C, top). Indeed, both serration and/or undulation and curling of leaves, associated with *NtKIS1a* and *AtCycD3;1* overexpression, respectively, disappeared in the crossed plants. Closer inspection of the restored phenotype was performed by scanning electron microscopy of leaf lower epidermis cells. Cell area measurement revealed that the three groups, previously described for WT plants (Fig. 4), were also represented in the AtCycD3;1×NtKIS1a plants (Fig. 6D). Indeed, in the crossed plants, cells with an area greater than 300 μm^2 reappeared compared with 35S::AtCycD3;1 plants and, reciprocally, cells with an area less than 3000 μm^2 reappeared compared with 35S::NtKIS1a plants (Fig. 4E; Fig. 6D). These results suggested an in vivo functional co-operation between these two cell cycle regulators.

Second, the *AtCycD3;1*-overexpressing line was transformed with the *NtKIS1a*-containing transgene, resulting in double overexpressing plants. The presence of the *NtKIS1a* transgene was controlled on genomic DNA in the Kanamycin-resistant (Km^R) T1 plantlets (AtCycD3;1+NtKIS1a) and its effective expression was monitored through RT-PCR analyses (Fig. 6B, right). As previously observed for crossed plants, double transformants displayed a WT-like phenotype (Fig. 6C, bottom). At the level of leaf lower epidermis cell area, the AtCycD3;1+NtKIS1a plants displayed a distribution similar to that found in crossed plants (not shown). Furthermore, the double transformed plants had an advanced flowering time

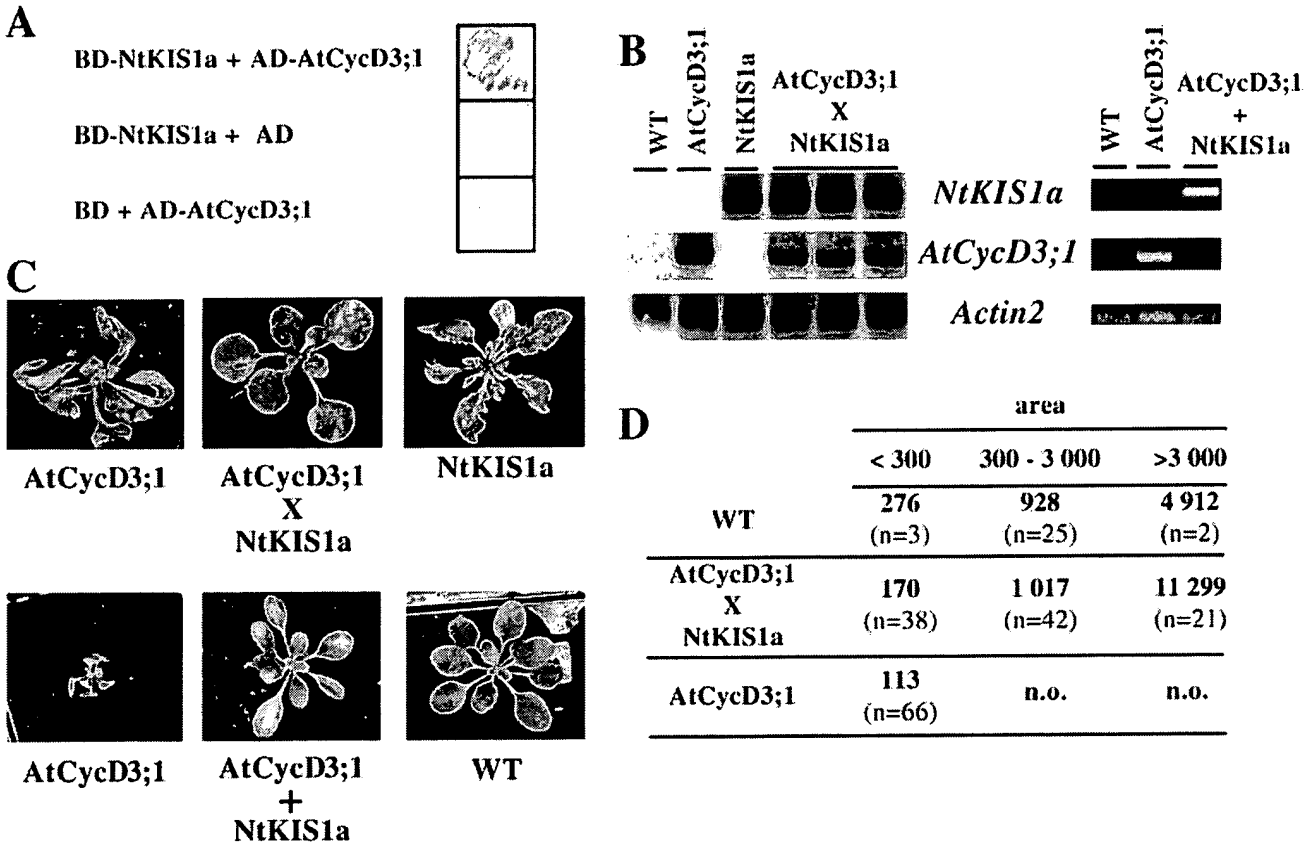

D

	area		
	< 300	300 - 3 000	>3 000
WT	276 (n=3)	928 (n=25)	4 912 (n=2)
AtCycD3;1 X NtKIS1a	170 (n=38)	1 017 (n=42)	11 299 (n=21)
AtCycD3;1	113 (n=66)	n.o.	n.o.

Fig. 6. *A. thaliana* plants overexpressing *NtKIS1a* and *AtCycD3;1* display a wildtype phenotype. (A) The interaction between NtKIS1a and AtCycD3;1 using the two-hybrid system is presented. BD-NtKIS1a corresponds to the DNA binding domain of GAL4 fused to NtKIS1a and AD-AtCycD3;1 corresponds to the activation domain of GAL4 fused to AtCycD3;1. AD and BD correspond respectively to the activation and DNA binding domains of GAL4. (B) RT-PCR analysis was performed as described in Materials and Methods. Lanes WT, AtCycD3;1, NtKIS1a, AtCycD3;1×NtKIS1a and AtCycD3;1+NtKIS1a are RT-PCR products obtained from RNA samples of the corresponding plants. AtCycD3;1×NtKIS1a correspond to the F1 plants of the cross between the AtCycD3;1 and NtKIS1a-overexpressing lines. AtCycD3;1+NtKIS1a correspond to T1 plants issued from the transformation of the AtCycD3;1-overexpressing line by the NtKIS1a-containing transgene. Three independent plants were tested for AtCycD3;1×NtKIS1a. PCR was performed with specific primers from *NtKIS1a* (first row), *AtCycD3;1* (second row) and *Actin2* (third row; used as control), respectively. (C) Top row: view of a 6-week-old plantlet from the *AtCycD3;1*-overexpressing line (AtCycD3;1), and view of 4-week-old plantlets from 35S::NtKIS1a (NtKIS1a) and AtCycD3;1×NtKIS1a lines. Bottom row: view of 3-week-old plantlets from *AtCycD3;1*-overexpressing line (AtCycD3;1), AtCycD3;1+NtKIS1a and WT. (D) From several scanning electron microscopy images of the lines described in C, bottom row, cell areas were measured using the Optimas 6.0 software. The averages of cell areas were reported in three categories, as described in the legend of Fig. 4. The measurement presented here for WT is an independent measurement of the WT measurement shown in Fig. 4.

compared with the flowering time of the 35S::AtCycD3;1 plants (Riou-Khamlichi et al., 1999) (not shown).

Since a wildtype-related phenotype was recovered through the combination of NtKIS1a and AtCycD3;1 by two independent manners, it strongly suggested that these two proteins, in addition to being two-hybrid interacting partners, co-operated in planta to restore a pseudo wildtype balance of their opposite activities towards cell cycle progression.

Discussion

Gain-of-function of NtKIS1a inhibits CDK kinase activity, cell division and disturbs plant morphology

Introduction of the tobacco CDK inhibitor NtKIS1a in *Arabidopsis* generated phenotypic modifications in several transgenic lines. Their phenotypic analysis demonstrated that the gain of function of NtKIS1a in *Arabidopsis* was correlated with an alteration of organ morphology (serration and/or undulation) together with a reduced plant growth, which resulted from the decrease in organ size (Fig. 1). In addition, 35S::NtKIS1a leaves contained larger cells than WT (Fig. 4) and our results indicated that more profound morphological alterations were associated with larger cells. Furthermore, in 35S::NtKIS1a extreme lines, organs such as petals, ovaries or anthers contained larger cells than in WT organs (Figs 2, 4). As a consequence of these observations, smaller organs must contain fewer cells. These results strongly suggested that NtKIS1a activity was sufficient to control organ and cell size as well as cell number. Since, cell number is determined primarily by cell division, the negative correlation between *NtKIS1a*

overexpression and organ cell number established that NtKIS1a, previously shown in vitro to be a CDK inhibitor (S.J., C.B. and N.G., unpublished), was also a negative regulator of cell division in planta. Indeed, it was confirmed that the kinase activity in 35S::NtKIS1a lines was strongly reduced, the level of inhibition being related to the strength of the phenotype (Fig. 2). The absence of phenotype in plants transformed with NtKIS1b, the NtKIS1a variant lacking inhibitory properties in vitro, correlated perfectly with the previous conclusions that established NtKIS1a as a negative cell cycle regulator. In mammals, $p27^{Kip1}$ was demonstrated to be a potent negative regulator of cell proliferation since mice lacking $p27^{Kip1}$ displayed enlarged organs that contained more cells (Fero et al., 1996). The decrease in cell number together with an increase in cell size in 35S::NtKIS1a organs may be viewed either as resulting from uncoupling of cell growth and cell division or as a direct correction by the morphogenetic programme to compensate for lack of cells (Meijer and Murray, 2001). Gain-of-function of the CDK inhibitor NtKIS1a was also associated with modifications in plant morphology, such as serration of leaves and petals (Figs 1, 4). This result suggested that plant organ shape could be disturbed solely by modulation of the *NtKIS1a* gene activity. Interestingly, overexpression of the *Arabidopsis* CKIs, *ICK1* (Wang et al., 2000), *KRP2* and *KRP3* (De Veylder et al., 2001), produced plant modifications closely related to overexpression of *NtKIS1a*. This suggested that the phenotypes observed reflected an overall effect of the constitutive overexpression of $p27^{Kip1}$-like CDK kinase inhibitors in *A. thaliana*, regardless of their specific function.

It was previously shown that depth of toothing or lobing could be affected by alteration of gibberellin levels (Chandra Sekhar and Sawhney, 1991). Investigation of such a relationship between NtKIS1a and gibberellins should be helpful to understand how *NtKIS1a* overexpression impaired leaf morphogenesis. Interestingly, there was a gradient in the strength of the serrated phenotype with deeper teeth in the strongest phenotype. Gradual modifications were observed in the T1 generation between normal plants, which were fertile and displayed only weakly serrated leaves, and the tiny extremely serrated plants displaying sterile flowers with short petals and non dehiscent anthers. It is important to note that abnormal flowers were never observed without strongly serrated leaves. It suggested that affecting cell division in petals required higher level of CKIs activity than needed for modifying leaf shape and size. Indeed, the analysis of the transgene disjunction demonstrated that the extreme phenotype affecting both leaves and flowers was only found in the strong T1 lines, where all the T2 progeny presented a serrated phenotype (Fig. 1C). It suggested that only the plants containing the highest number of transgene copies were affected in flowers. Remarkably, in 35S::NtKIS1a plants, all organs were formed with the right identity. Therefore, despite *NtKIS1a* being expressed under the constitutive 35S promoter, it did not interfere with identity acquisition of meristems nor organs. NtKIS1a would preferentially act at terminal differentiation of the plant organ cells since only the morphogenesis of organs was affected.

Cell size and endoreduplication

There is a large body of evidence indicating that the final size of a cell is linked to its DNA content (Traas et al., 1998). In 35S::NtKIS1a rosette leaves, cells displayed a 2C and 4C DNA content distribution (Fig. 5), demonstrating that the endoreduplication phenomenon, known to occur in the WT rosette, was affected. Interestingly, in the 35S::NtKIS1a plants, which displayed a strong serrated phenotype, endoreduplication was completely prevented (Fig. 5), whereas this block was only partial in less affected plants (medium and weak lines, not shown). This result demonstrated that the NtKIS1a CDK inhibitor interfered with the endoreduplication phenomenon in *Arabidopsis* when overexpressed. However, these results did not provide information towards the involvement of NtKIS1a in endoreduplication in tobacco. Surprisingly, the endoreduplication block observed in *NtKIS1a*-overexpressing *Arabidopsis* was accompanied with a phenomenal cell enlargement: 6.3-fold in the strong lines in which the endoreduplication block was complete (Figs 4, 5). It demonstrated that, in 35S::NtKIS1a *Arabidopsis* rosette leaves, endoreduplication and cell size could be uncoupled.

Endoreduplication and differentiation

Endoreduplication is the major mechanism leading to somatic polyploidisation in plants and has been described in many specific cell types that are highly specialised (Joubes and Chevalier, 2000). This phenomenon represents a growing field of interest in plant biology as it characterises the switch between cell proliferation and cell differentiation during developmental steps. Endoreduplication shares several characteristics with the mitotic cycle. In particular, the endoreduplicative cycle appears to be under control of the same CDK/cyclin complexes. However, both cycles are mutually exclusive and higher eukaryotes have developed strategies that ensure an inhibition of endoreduplication during mitosis and vice versa (Larkins et al., 2001). A variety of biological processes, especially cell differentiation, have been proposed to involve endoreduplication (Joubes and Chevalier, 2000). However, the role and the control of the endocycle are poorly characterised in plants. Interestingly, since two plant CKIs [*NtKIS1a* (this paper) and *KRP2* (De Veylder et al., 2001)] prevented endoreduplication when overexpressed, it suggested that CKIs could be potent regulators of this phenomenon in *Arabidopsis*. Similarly, in *Caenorhabditis elegans*, it was suggested that the CDK inhibitor CKI-1 might play a role in endoreduplication, since it was expressed in differentiated intestinal cells that underwent endoreduplicative cell cycles (Hong et al., 1998). In mammals, $p57^{Kip2}$ is involved in the transition to the endocycle in trophoblast giant cells during terminal differentiation and interestingly, ectopic expression of a stabilised $p57^{Kip2}$ mutant protein blocked endoreduplication (Hattori et al., 2000). Furthermore, the mutation of the CDK and cyclin binding domains of $p57^{Kip2}$ abrogated its inhibitory activity on endoreduplication when overexpressed (Hattori et al., 2000). Consistent with this, endoreduplication occurred in plants overexpressing *NtKIS1b* (Fig. 5), which lacked the C-terminal end, necessary for both CDK and cyclin interaction (S.J., C.B. and N.G., unpublished).

NtKIS1a and cyclin D3;1 interaction

In mammals, D-cyclins are thought to drive cell cycle

progression by associating with their CDK partners (CDK4 and CDK6) and by guiding these kinases to their cellular substrates (Sherr, 1995). In addition to their well-documented CDK-dependent role, D-cyclins play a kinase independent function by sequestering cell cycle inhibitors $p27^{Kip1}$ and $p21^{Cip1}$, thereby triggering the kinase activity of cyclin E-CDK2 (Sherr and Roberts, 1999). Moreover, in the context of a living mouse, the significance of cyclin D1-$p27^{Kip1}$ interaction was demonstrated, since deletion of $p27^{Kip1}$ rescues developmental abnormalities of cyclin D1-deficient mice (Geng et al., 2001; Tong and Pollard, 2001). NtKIS1a was shown to interact with tobacco and *Arabidopsis* D-cyclins (S.J., C.B. and N.G., unpublished) (Fig. 6A), known as positive regulators of the cell cycle machinery (De Veylder et al., 1999; Riou-Khamlichi et al., 1999; Riou-Khamlichi et al., 2000). In order to address the significance of cyclin D-NtKIS1a interaction in the context of a living *Arabidopsis*, *AtCycD3;1* (Riou-Khamlichi et al., 1999) and *NtKIS1a* were overexpressed simultaneously in plants in two ways. Our phenotypic analyses revealed that overexpression of *NtKIS1a* together with *AtCycD3;1* restored normal plant development. Regarding the leaf phenotype, both the serration and/or undulation observed in NtKIS1a lines and the curling of AtCycD3;1 line disappeared in double overexpressing plants (Fig. 6C). This leaf phenotype restoration was also confirmed at the cellular level, since in double overexpressing plants, cell areas could be described by three categories such as in WT (Fig. 4E; Fig. 6D). Furthermore, several other traits were addressed in the double overexpressing plants (cell shape, plant and organ size, flowering time; not shown) and all converged on the WT phenotype restoration. Consequently, one interpretation would be that the enhanced inhibitory activity brought by *NtKIS1a* overexpression, would allow compensation of the hyperproliferative properties associated with *AtCycD3;1* overexpression. As already mentioned above for animals, D-cyclins control the activity of CDK/cyclin E, responsible for S phase entry, via titration of CIP/KIP (Sherr and Roberts, 1999). Although E-cyclins have not yet been found in plants, a member of the D-cyclin family (cyclin δ2) has some characteristics in common with E-cyclins (Soni et al., 1995). Thus, a second interpretation could be that NtKIS1a would be sequestrated by AtCycD3;1, allowing the activation of putative E-cyclins and then re-activation of mitotic activity. To summarise, our findings indicate that NtKIS1a and AtCycD3;1 function to antagonise each other and this represents the first demonstration in planta of co-operation between a cell cycle inhibitor, NtKIS1a, and a cell cycle activator, AtCycD3;1.

We are grateful to P. Ratet for providing the *Agrobacterium tumefaciens* strain HBA10S, to C. Gatz for providing the Bin-Hyg-TX vector and to O. Grandjean for allowing us the access to the optimas 6.0 software. We thank J. A. H. Murray and R. Stevens for their critical reading of the manuscript, M. Delarue for her helpful criticisms, J. P. Barès and G. Santé for taking care of the plants and R. Boyer for photography. S.G. was supported by a grant from the French MENRT.

References

Azzi, L., Meijer, L., Reed, S. I., Pidikiti, R. and Tung, H. Y. (1992). Interaction between the cell-cycle-control proteins p34cdc2 and p9CKShs2. Evidence for two cooperative binding domains in p9CKShs2. *Eur. J. Biochem.* **203**, 353-360.

Bechtold, N. and Pelletier, G. (1998). In planta Agrobacterium-mediated transformation of adult *Arabidopsis thaliana* plants by vacuum infiltration. *Methods Mol. Biol.* **82**, 259-266.

Bergounioux, C., Brown, S. C. and Petit, P. X. (1992). Flow cytometry and plant protoplast cell biology. *Physiol. Plant.* **85**, 374-386.

Chandra Sekhar, K. N. and Sawhney, V. K. (1991). Regulation of leaf shape in the solanifolia mutant of tomato (*Lycopersicon esculentum*) by plant growth substances. *Ann. Bot.* **67**, 3-6.

Chen, I. T., Akamatsu, M., Smith, M. L., Lung, F. D., Duba, D., Roller, P. P., Fornace, A. J., Jr and O'Connor, P. M. (1996). Characterization of p21Cip1/Waf1 peptide domains required for cyclin E/Cdk2 and PCNA interaction. *Oncogene* **12**, 595-607.

Church, G. M. and Gilbert, W. (1984). Genomic sequencing. *Proc. Natl. Acad. Sci. USA* **81**, 1991-1995.

Cobrinik, D., Lee, M. H., Hannon, G., Mulligan, G., Bronson, R. T., Dyson, N., Harlow, E., Beach, D., Weinberg, R. A. and Jacks, T. (1996). Shared role of the pRB-related p130 and p107 proteins in limb development. *Genes Dev.* **10**, 1633-1644.

De Veylder, L., de Almeida Engler, J., Burssens, S., Manevski, A., Lescure, B., Van Montagu, M., Engler, G. and Inze, D. (1999). A new D-type cyclin of *Arabidopsis thaliana* expressed during lateral root primordia formation. *Planta* **208**, 453-462.

De Veylder, L., Beeckman, T., Beemster, G. T., Krols, L., Terras, F., Landrieu, I., van der Schueren, E., Maes, S., Naudts, M. and Inze, D. (2001). Functional analysis of cyclin-dependent kinase inhibitors of *Arabidopsis*. *Plant Cell* **13**, 1653-1668.

Fero, M. L., Rivkin, M., Tasch, M., Porter, P., Carow, C. E., Firpo, E., Polyak, K., Tsai, L. H., Broudy, V., Perlmutter, R. M. et al. (1996). A syndrome of multiorgan hyperplasia with features of gigantism, tumorigenesis, and female sterility in p27(Kip1)-deficient mice. *Cell* **85**, 733-744.

Galbraith, D. W., Harkins, K. R., Maddox, J. M., Ayres, N. M., Sharma, D. P. and Firoozabady, E. (1983). Rapid flow cytometric analysis of the cell cycle in intact plant tissues. *Science* **220**, 1049-1051.

Geng, Y., Yu, Q., Sicinska, E., Das, M., Bronson, R. T. and Sicinski, P. (2001). Deletion of the p27Kip1 gene restores normal development in cyclin D1- deficient mice. *Proc. Natl. Acad. Sci. USA* **98**, 194-199.

Hattori, N., Davies, T. C., Anson-Cartwright, L. and Cross, J. C. (2000). Periodic expression of the cyclin-dependent kinase inhibitor p57(Kip2) in trophoblast giant cells defines a G2-like gap phase of the endocycle. *Mol. Biol. Cell* **11**, 1037-1045.

Hong, Y., Roy, R. and Ambros, V. (1998). Developmental regulation of a cyclin-dependent kinase inhibitor controls postembryonic cell cycle progression in Caenorhabditis elegans. *Development* **125**, 3585-3597.

Joubes, J. and Chevalier, C. (2000). Endoreduplication in higher plants. *Plant Mol. Biol.* **43**, 735-745.

Koornneef, M. (1994). General genetics. In *Arabidopsis* (ed. E. M. Meycrowitz and C. R. Somerville), pp. 89-120. Plainview, NY: Cold Spring Harbor Laboratory Press.

Larkins, B. A., Dilkes, B. P., Dante, R. A., Coelho, C. M., Woo, Y. and Liu, Y. (2001). Investigating the hows and whys of DNA endoreduplication. *J. Exp. Bot.* **52**, 183-192.

Meijer, M. and Murray, J. A. H. (2000). The role and regulation of D-type cyclins in the plant cell cycle. *Plant Mol. Biol.* **43**, 621-633.

Meijer, M. and Murray, J. A. (2001). Cell cycle controls and the development of plant form. *Curr. Opin. Plant Biol.* **4**, 44-49.

Myster, D. L. and Duronio, R. J. (2000). To differentiate or not to differentiate? *Curr. Biol.* **10**, 302-304.

Ohnuma, S., Philpott, A., Wang, K., Holt, C. E. and Harris, W. A. (1999). p27Xic1, a Cdk inhibitor, promotes the determination of glial cells in *Xenopus* retina. *Cell* **99**, 499-510.

Riou-Khamlichi, C., Huntley, R., Jacqmard, A. and Murray, J. A. (1999). Cytokinin activation of *Arabidopsis* cell division through a D-type cyclin. *Science* **283**, 1541-1544.

Riou-Khamlichi, C., Menges, M., Healy, J. M. and Murray, J. A. (2000). Sugar control of the plant cell cycle: differential regulation of *Arabidopsis* D-type cyclin gene expression. *Mol. Cell Biol.* **20**, 4513-4521.

Russo, A. A., Jeffrey, P. D., Patten, A. K., Massague, J. and Pavletich, N. P. (1996). Crystal structure of the p27Kip1 cyclin-dependent-kinase inhibitor bound to the cyclin A-Cdk2 complex. *Nature* **382**, 325-331.

Sherr, C. J. (1995). D-type cyclins. *Trends Biochem. Sci.* **20**, 187-190.

Sherr, C. J. and Roberts, J. M. (1999). CDK inhibitors: positive and negative regulators of G1-phase progression. *Genes Dev.* **13**, 1501-1512.

Sicinski, P., Donaher, J. L., Parker, S. B., Li, T., Fazeli, A., Gardner, H., Haslam, S. Z., Bronson, R. T., Elledge, S. J. and Weinberg, R. A. (1995). Cyclin D1 provides a link between development and oncogenesis in the retina and breast. *Cell* **82**, 621-630.

Soni, R., Carmichael, J. P., Shah, Z. H. and Murray, J. A. (1995). A family of cyclin D homologs from plants differentially controlled by growth regulators and containing the conserved retinoblastoma protein interaction motif. *Plant Cell* **7**, 85-103.

Stals, H. and Inze, D. (2001). When plant cells decide to divide. *Trends Plant. Sci.* **6**, 359-364.

Tong, W. and Pollard, J. W. (2001). Genetic evidence for the interactions of cyclin D1 and p27(Kip1) in mice. *Mol. Cell Biol.* **21**, 1319-1328.

Traas, J., Hulskamp, M., Gendreau, E. and Hofte, H. (1998). Endoreduplication and development: rule without dividing? *Curr. Opin. Plant Biol.* **1**, 498-503.

Trehin, C., Planchais, S., Glab, N., Perennes, C., Tregear, J. and Bergounioux, C. (1998). Cell cycle regulation by plant growth regulators: involvement of auxin and cytokinin in the re-entry of Petunia protoplasts into the cell cycle. *Planta* **206**, 215-224.

Wang, H., Qi, Q., Schorr, P., Cutler, A. J., Crosby, W. L. and Fowke, L. C. (1998). ICK1, a cyclin-dependent protein kinase inhibitor from *Arabidopsis thaliana* interacts with both Cdc2a and CycD3, and its expression is induced by abscisic acid. *Plant J.* **15**, 501-510.

Wang, H., Zhou, Y., Gilmer, S., Whitwill, S. and Fowke, L. C. (2000). Expression of the plant cyclin-dependent kinase inhibitor ICK1 affects cell division, plant growth and morphology. *Plant J.* **24**, 613-623.

Zhang, P., Wong, C., DePinho, R. A., Harper, J. W. and Elledge, S. J. (1998). Cooperation between the Cdk inhibitors p27(KIP1) and p57(KIP2) in the control of tissue growth and development. *Genes Dev.* **12**, 3162-3167.

Zhang, P., Wong, C., Liu, D., Finegold, M., Harper, J. W. and Elledge, S. J. (1999). p21(CIP1) and p57(KIP2) control muscle differentiation at the myogenin step. *Genes Dev.* **13**, 213-224.

The Plant Cell, Vol. 13, 1653–1667, July 2001, www.plantcell.org © 2001 American Society of Plant Biologists

Functional Analysis of Cyclin-Dependent Kinase Inhibitors of Arabidopsis

Lieven De Veylder,[a] Tom Beeckman,[a] Gerrit T. S. Beemster,[a] Luc Krols,[b] Franky Terras,[b] Isabelle Landrieu,[c] Els Van Der Schueren,[a] Sara Maes,[a] Mirande Naudts,[a] and Dirk Inzé[a,1]

[a] Vakgroep Moleculaire Genetica, Departement Plantengenetica, Vlaams Interuniversitair Instituut voor Biotechnologie, Universiteit Gent, K.L. Ledeganckstraat 35, B-9000 Gent, Belgium

[b] CropDesign N.V., B-9052 Zwijnaarde, Belgium

[c] Institut de Biologie de Lille/Institut Pasteur de Lille, Centre National de la Recherche Scientifique Unité Mixte de Recherche 8525, F-59019 Lille Cedex, France

Cyclin-dependent kinase inhibitors, such as the mammalian p27^{Kip1} protein, regulate correct cell cycle progression and the integration of developmental signals with the core cell cycle machinery. These inhibitors have been described in plants, but their function remains unresolved. We have isolated seven genes from Arabidopsis that encode proteins with distant sequence homology with p27^{Kip1}, designated Kip-related proteins (KRPs). The KRPs were characterized by their domain organization and transcript profiles. With the exception of KRP5, all presented the same cyclin-dependent kinase binding specificity. When overproduced, KRP2 dramatically inhibited cell cycle progression in leaf primordia cells without affecting the temporal pattern of cell division and differentiation. Mature transgenic leaves were serrated and consisted of enlarged cells. Although the ploidy levels in young leaves were unaffected, endoreduplication was suppressed in older leaves. We conclude that KRP2 exerts a plant growth inhibitory activity by reducing cell proliferation in leaves, but, in contrast to its mammalian counterparts, it may not control the timing of cell cycle exit and differentiation.

INTRODUCTION

Growth is one of the most studied phenomena in multicellular organisms. It has become clear that the process of cell division plays a crucial role in the mechanisms by which higher organisms achieve appropriate development of their organs. The cell division cycle is controlled by a molecular machinery that ensures the fidelity of DNA replication and that responds to signals from both the external environment and intrinsic developmental programs. A central role in the regulation of the cell cycle is played by the cyclin-dependent kinases (CDKs). CDK activity is controlled by a variety of mechanisms, including binding to cyclins (for review, see Pines, 1994) and phosphorylation of the Thr-161 (or an equivalent) residue by the CDK-activating kinase (for review, see Dunphy, 1994).

Active cyclin/CDK complexes can be inhibited in different ways. The phosphorylation of the Thr-14 and Tyr-15 residues interferes with the correct binding of the cofactor ATP and, therefore, inhibits CDK activity (Dunphy, 1994). Indirectly, kinase activity also is inhibited by the controlled degradation of cyclin subunits (for review, see Peters, 1998). Recently, another mechanism of the negative regulation of CDK activity has become evident. A family of mainly low-molecular-weight proteins, named CDK inhibitors (CKIs), inhibit CDK activity by tight association with the cyclin/CDK complexes (for review, see Sherr and Roberts, 1995, 1999). In mammals, two different CKI families can be distinguished on the basis of their mode of action and sequence similarity: the INK4 and the Kip/Cip families.

The Kip/Cip family comprises three gene products: p21^{Cip1}, p27^{Kip1}, and p57^{Kip2}. These CKIs bind to all known G1/S-specific CDKs (Toyoshima and Hunter, 1994; Lee et al., 1995). The Kip/Cip CKIs are involved in both checkpoint control and the regulation of cell cycle exit preceding differentiation. The former function is illustrated by the observed association of p21^{Cip1} with CDKs in a p53-dependent manner upon the occurrence of DNA damage, inhibiting replication but still allowing DNA repair (Dulić et al., 1994; Smith et al., 1994). A role of the CKIs in cell differentiation is seen during muscle development. Mice lacking both p21^{Cip1} and p57^{Kip2} display severe defects in skeletal muscle development because of prolonged proliferation and inhibited differentiation (Zhang et al., 1999). Moreover, p27^{Kip1} has been implicated as a mediator of various antimitogenic stimuli

[1] To whom correspondence should be addressed. E-mail diinz@gengenp.rug.ac.be; fax 32-9-2645349.

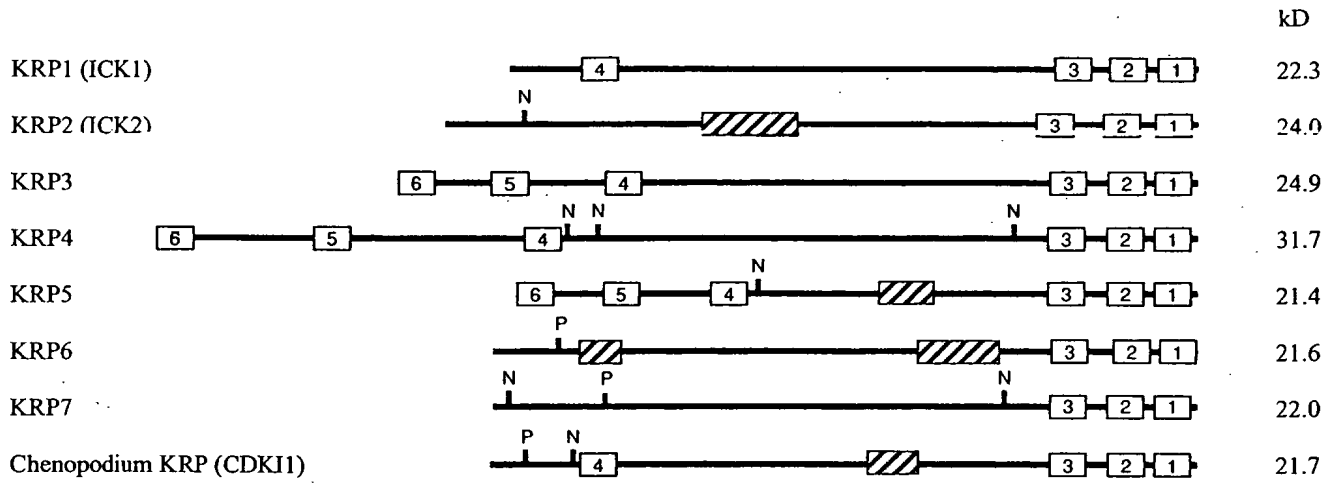

Figure 1. Structural Organization of KRP1, KRP2, KRP3, KRP4, KRP5, KRP6, KRP7, and Chenopodium KRP.

Conserved sequence boxes are indicated (1 to 6). N, nuclear localization signal; P, CDK consensus phosphorylation site; striped boxes, PEST domains. The predicted molecular masses (kD) are indicated at right.

(Kato et al., 1994; Nourse et al., 1994; Polyak et al., 1994). Kip1 nullizygous mice are significantly larger than control mice because of an increase in the number of cells, suggesting that the absence of $p27^{Kip1}$ might allow continued cell proliferation in the presence of antimitogenic signals (Fero et al., 1996; Nakayama et al., 1996).

A novel function for the Kip/Cip CKIs has been revealed by the observation that $p21^{Cip1}$ and $p27^{Kip1}$ associate with active cyclin D/CDK4 complexes (LaBaer et al., 1997). Not only are the cyclin D/CDK4 complexes inert toward the inhibitory function of the Kip/Cip proteins, but their activation is stimulated by the CKIs (Cheng et al., 1999). Because the Kip/Cip proteins contain interaction sites with both cyclin D and CDK subunits, they help assemble the cyclin D/CDK complexes. In addition, the CKIs direct the cyclin D/CDK complexes to the nucleus, where they are phosphorylated by the CDK-activating kinase.

In plants, two major groups of CDKs have been studied: the A-type and B-type CDKs (Mironov et al., 1999). The A-type CDKs, represented by CDKA;1 (previously designated CDC2aAt; Joubès et al., 2000) in Arabidopsis, show kinase activity during the S, G2, and M phases of the cell cycle. In contrast, the activity of B-type CDKs, represented by CDKB1;1 (previously designated CDC2bAt) in Arabidopsis, is linked prominently to mitosis (Magyar et al., 1997; our unpublished results). These data indicate that A-type CDKs regulate both the G1-to-S and G2-to-M transitions, whereas the B-type CDKs regulate the G2-to-M transition only. Downregulation of A-type CDK activity in plants does not affect the relative duration of G1 and G2. In contrast, plants with reduced B-type CDK activity have an increased duration of G2 (Hemerly et al., 1995; our unpublished results).

To date, only two structurally related CKI-like molecules have been described for plants, ICK1 and ICK2 (Wang et al.,

Table 1. Conserved Motifs in the Plant KRPs

Protein	Motif 1	Motif 2	Motif 3	Motif 4	Motif 5	Motif 6
KRP1	180-PLEGRYEW	167-FKKKYNFD	151-EIEDFFVEAE	20-YMQLRSRR		
KRP2	197-LGGGRYEW	183-CSMKYNFD	164-ELEDFFQVAE			
KRP3	210-PLSGRYEW	197-FMEKYNFD	181-EMEEFFAYAE	58-YLQLRSRR	26-SPGVRTRA	1-MGKYMKKSK
KRP4	274-PLPGRFEW	261-FIEKYNFD	245-EMDEFFSGAE	102-YLQLRSRR	44-SLGVLTRA	1-MGKYIRKSK
KRP5	177-PLPGRYEW	164-FIQKYNFD	148-EIEDFFASAE	54-YLQLRSRR	24-ALGFRTRA	1-MGKYIKKSK
KRP6	186-PLEGRYKW	173-FIEKYNFD	155-EIEDLFSELE			
KRP7	183-PLEGRYQW	170-FTEKYNYD	154-ELDDFFSAAE			
CDKI1[a]	184-PLKGRYDW	171-FSEKYNFD	155-EIEEFFAVAE	25-IPQLRSRR		

[a] Chenopodium KRP.

1997; Lui et al., 2000). Interestingly, ICK1 was demonstrated to be twofold to threefold transcriptionally induced upon abscisic acid treatment, suggesting that this CKI might be responsible for the growth inhibitory effect of abscisic acid (Wang et al., 1998). Despite their low sequence identity with the mammalian Kip/Cip inhibitors, recombinant ICK1 and ICK2 proteins inhibited CDK activity in an in vitro assay (Wang et al., 1997; Lui et al., 2000). Recently, the CDK inhibitory activity of ICK1 was demonstrated by its overproduction in Arabidopsis, resulting in dwarf plants with a reduced number of cells that were much larger than those of wild-type plants (Wang et al., 2000).

Here we report the existence of five additional *CKI* genes in Arabidopsis. We show that (1) the various *CKI* genes are expressed differentially, whereas their gene products, with the exception of the Kip-related protein 5, all bind the same CDK; (2) the reduced cell number and size of CKI transgenic plants are a consequence of inhibited cell division and leaf expansion rates, whereas the temporal pattern of development is unaffected; and (3) the rate of endoreduplication is inhibited as well.

RESULTS

Cloning of p27^{Kip1}-Like Genes from Arabidopsis

To investigate the presence and function of plant CKIs, a two-hybrid screen was performed with the Arabidopsis CDKA;1. Among the interacting clones, three putative CKIs were identified, two of which were identical to the *ICK1* and *ICK2* genes described previously (Wang et al., 1997; Lui et al., 2000). In parallel, we identified four related genes in the Arabidopsis genomic databases, of which the cDNAs were isolated by reverse transcriptase–mediated polymerase chain reaction (PCR). Because all proteins showed sequence identity to the mammalian p27^{Kip1} CKI in their C-terminal domains, we propose to name these proteins Kip-related proteins (KRPs) with the numbers 1 to 7, where KRP1 and KRP2 correspond to ICK1 and ICK2, respectively. Overall, the KRPs have no significant sequence identity to any proteins in the databases. They also display only low sequence identity to each other. However, a detailed analysis allowed us to identify small sequence elements shared by different KRP members (Figure 1, Table 1).

Three domains located at the extremity of the C-terminal part of the proteins are shared by all KRPs and are found in a CKI-like molecule from *Chenopodium rubrum*. Only the two last motifs are present in mammalian CKIs such as p27^{Kip1}. The other three domains are not common among all of the KRPs but were identified in at least two different members of the KRP family. A motif 3–related sequence (ELDEFFAEAE) is shared with the erythronolide synthase from *Streptomyces erythraeus*, and a motif 6–related sequence (SLGFLTRA) is located in the TPR1 protein of fission yeast, which is involved in potassium transport. However, the significance of these motifs is unknown. Motifs 4 and 6 share no similarity with any protein in the databases. In addition to the motifs mentioned above, KRP2, KRP5, and KRP6 all have PEST domains (PESTfind score $> +10$), which are polypeptide sequences enriched in proline (P), glutamic acid (E), serine (S), and threonine (T) residues that serve as proteolytic signals (Rogers et al., 1986) (Figure 1). Furthermore, KRP2, KRP4, KRP5, and KRP7 carry at least one nuclear localization signal (Figure 1). Finally, KRP6 and KRP7 can be distinguished from other KRPs by the presence of a consensus CDK phosphorylation site (S/TPXK/R) in their N-terminal domains (Figure 1).

KRPs Do Not Bind the Mitotic CDKB1;1

KRP1 and KRP2 have been shown to interact with CDKA;1 but not with CDKB1;1 in a two-hybrid system (Lui et al., 2000). We tested the binding specificity for all identified KRPs toward the same CDKs. Plasmids that encode the CDKA;1 or CDKB1;1 protein fused to the GAL4 DNA binding domain (GAL4-BD) were cotransformed in a yeast reporter strain with vectors that encode a fusion protein between the different KRPs and the GAL4 activation domain (GAL4-AD). Transformants were streaked on medium lacking histidine, because the yeast reporter strain would grow only in the absence of histidine when the proteins interacted. As summarized in Table 2, all KRPs, except KRP5 and KRP6, interacted with CDKA;1, and none interacted with CDKB1;1. In contrast, the CDK docking factor CKS1At interacted with both CDKs, demonstrating that CDKB1;1 was functional in our two-hybrid assay. In a reciprocal two-hybrid experiment in which the KRPs and CDKs were cloned as fusion proteins with the GAL4-BD and GAL4-AD, respectively, KRP6 also interacted with CDKA;1 (Table 2). This interaction might be attributable to the fusion between KRP6 and the GAL4-BD being more stable than that with the GAL4-AD. The KRP1, KRP2, and KRP3 proteins could not be used in this assay

Table 2. Interaction of KRPs with CDKA;1, CDKB1;1, and CYCD4

	CDKA;1		CDKB1;1		CYCD4
Prey/Bait[a]	GAL-BD	GAL-AD	GAL-BD	GAL-AD	GAL-AD
KRP1	+		−		
KRP2	+		−		
KRP3	+		−		
KRP4	+	+	−	−	+
KRP5	−	−	−	−	+
KRP6	−	+	−	−	+
KRP7	+	+	−	−	+
CKS1At	+	+	+	+	−

[a] Depending on the CDK-containing construct.

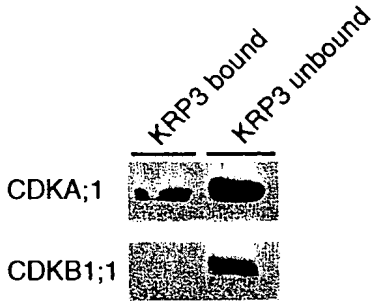

Figure 2. In Vitro CDKA;1 Binding by KRP3.

Protein extracts of 3-day-old cell suspensions of Arabidopsis were loaded onto a KRP3-Sepharose column, and bound and unbound fractions were tested for the presence of CDKA;1 or CDKB1;1 with specific antibodies.

because the fusion of these proteins with the GAL4-BD activated the reporter gene in the absence of a prey. Thus, except for KRP5, all KRPs bound specifically with CDKA;1.

For KRP3, the binding specificity toward CDKA;1 was confirmed by an in vitro assay. The recombinant KRP3 protein was synthesized in *Escherichia coli* and purified to homogeneity. The purified protein was coupled to Sepharose beads, which were used to make an affinity column. To this column, total Arabidopsis cell suspension extracts were applied. Both the unbound and bound protein fractions were separated subsequently by electrophoresis and transferred to membranes. Afterward, these membranes were probed with CDKA;1- and CDKB1;1-specific antibodies. As can be seen in Figure 2, CDKA;1 was detected in the flow-through fraction, but a significant amount also was bound to the column, indicating again a stable interaction between KRP3 and CDKA;1. In contrast, the CDKB1;1 protein was detected only in the flow-through fraction.

The mammalian Cip/Kip family members interact with both the CDK and cyclin subunits. Accordingly, the KRP1 protein was shown to interact with the D-type cyclin CYCD3 from Arabidopsis (Wang et al., 1998). Here we tested the interaction of the KRPs with CYCD4 (De Veylder et al., 1999). As seen in Table 2, all KRPs tested, including KRP5, interacted with this particular cyclin. These results show that the inability of KRP5 to interact with CDKA;1 was not caused by the instability of the protein in yeast and suggest that KRP5 binds to a yet-unidentified CDK from Arabidopsis that can make a complex with CYCD4.

The *KRP* Genes Are Expressed Differentially in Plant Tissues

The expression of the different *KRP* genes in various plant organs (roots, inflorescence stems, flower buds, and 3-week-old leaves) and in a 3-day-old, actively dividing suspension culture was studied by semiquantitative reverse transcriptase–mediated PCR because not all of the genes were expressed strongly enough to be detected by classic RNA gel blotting. PCR was performed with a specific primer set for each of the KRPs (see Methods). Amplification with actin 2–specific primers was used to ensure equal input of cDNA for each sample. As can be seen in Figure 3, only *KRP1* and *KRP6* were expressed ubiquitously. *KRP4*, *KRP5*, and *KRP7* were detected in all tissues, but mRNA clearly was more abundant in the tissues that displayed high mitotic activity (flowers and suspension cultures), with *KRP4* also being abundantly present in leaves. *KRP2* was most abundant in flowers. Remarkably, the expression of *KRP3* was particularly high in actively dividing suspension cultures but was not, or was barely (in roots and flowers), detectable

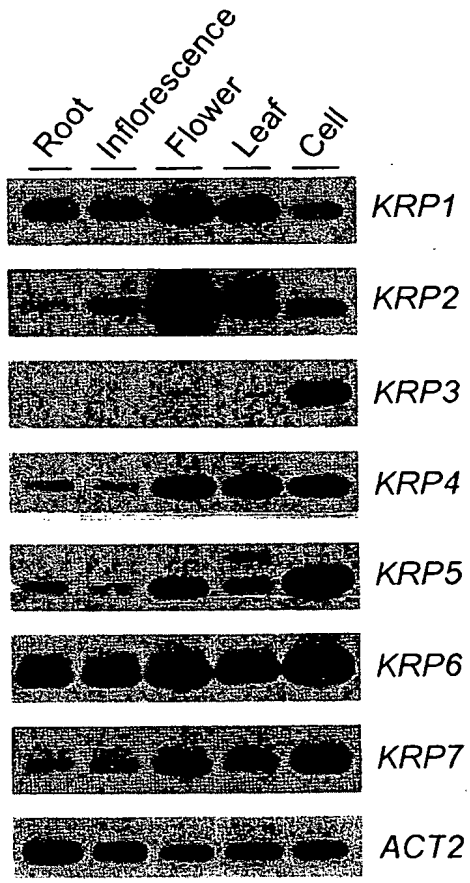

Figure 3. Differential Expression of *KRP* Genes in Various Arabidopsis Organs and a 3-Day-Old Cell Suspension Culture.

cDNA prepared from the indicated organs and the suspension cell culture were subjected to semiquantitative reverse transcriptase–mediated PCR analysis using gene-specific primers (see Methods). The actin 2 gene (*ACT2*) was used as a loading control.

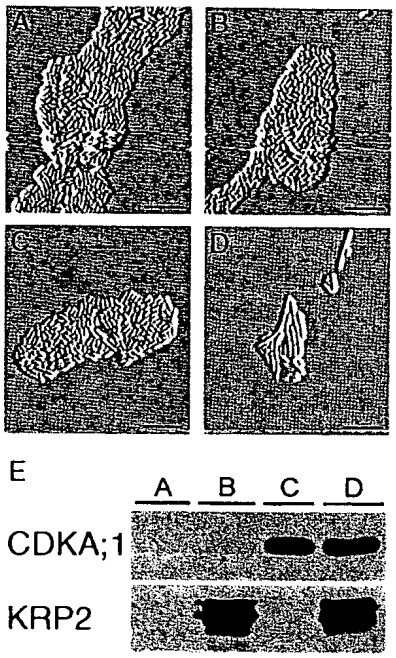

Figure 4. KRP2 Inhibition of Advanced Mitosis in Yeast Caused by the *CDKA;1.A14F15* Gene.

(A) Wild-type fission yeast cells transformed with empty control vectors.
(B) Yeast cells expressing the *KRP2* gene.
(C) Yeast cells expressing the dominant positive *CDKA;1.A14F15* gene.
(D) Yeast cells coexpressing the *CDKA;1.A14F15* and *KRP2* genes.
(E) Protein gel blot analysis of protein levels of CDKA;1 and KRP2 in the cells from **(A)** to **(D)**.
Bars in **(A)** to **(D)** = 30 μm.

in intact plant organs. The organ-specific expression patterns of *KRP1* and *KRP2* corresponded with those reported previously by Lui et al. (2000), although minor differences in the amount of transcript accumulation were observed that may be explained by differences in time of harvesting the plant material. Together, the transcription profiles suggest that the various KRPs might play distinct roles in plant development.

Inhibition of CDKA;1 Activity by KRPs in Yeast

To test the CKI activity of the KRPs in vivo, a genetic experiment in fission yeast was designed. In this assay, CDK inhibition was evaluated as the potential to convert prematurely dividing cells into noncycling cells. The assay is illustrated here for the KRP2 protein, but similar results were obtained for the other KRP proteins tested (KRP1 and KRP4). As illustrated in Figure 4, yeast cells that expressed the *KRP2* gene exhibited no growth abnormalities or changes in cell morphology compared with control cells (Figures 4A, 4B, and 4E), demonstrating that the expression of *KRP2* did not inhibit the cell cycle of yeast. This result is not surprising, because the KRP2 protein is entirely unrelated to any of the known CKIs from yeast. In contrast, cells that expressed a dominant positive allele of the *CDKA;1* gene (*CDKA;1.A14F15*) divided prematurely, resulting in cells being slightly smaller than control cells (Figures 4A, 4C, and 4E). It has been demonstrated previously that this reduced cell size results from an increase of the total CDK activity in the yeast cells (Porceddu et al., 1999) and that *CDKA;1.A14F15* is expected to sequester the majority of the yeast cyclins. However, when the mutant *CDKA;1* allele was coexpressed with *KRP2*, cells were much longer than those of the wild type (Figures 4D and 4E), indicating cell cycle arrest. The most probable explanation for this cell cycle arrest is the conversion by the KRP2 protein of the dominant positive form of CDKA;1 into an inactive form. In any case, these data show indirectly the potential of KRP2 to inhibit specifically plant CDK activity.

KRP Overexpression in Plants

To analyze the roles of the KRPs in plant development, we generated transgenic plants containing the *KRP1*, *KRP2*, *KRP3*, or *KRP4* gene under the control of the constitutive cauliflower mosaic virus 35S promoter. For *KRP4*, no transgenic lines could be obtained, although several independent transformations were undertaken. In contrast, numerous independent transgenic lines were generated for *KRP1*, *KRP2*, and *KRP3*. Here we report in detail the phenotype of the KRP2-overproducing lines.

Thirty-nine lines were generated in which the levels of the *KRP2* mRNA and the KRP2 protein exceeded those found in untransformed plants (Figures 5A and 5B). The presence of the KRP2 protein correlated with a decrease in extractable CDK activity (Figures 5E and 5F). Remarkably, the overproduction of KRP2 led to an increase in CDKA;1 protein level (Figure 5C). No change in the *CDKA;1* mRNA level was observed (data not shown), indicating that overproduction of the KRP2 protein may stabilize the CDKA;1 protein.

KRP2-overproducing plants had narrower leaves than did wild-type plants. As reported for the overproduction of KRP1 (Wang et al., 2000), the leaves of KRP2-overproducing plants were distinctly serrated (Figures 6A to 6D). In addition, sepals and petals were modified in size, and flowers were partially male sterile. Furthermore, the number of lateral roots appeared to be reduced by ~50%. There was no obvious effect on stem size, root elongation rate, and hypocotyl length (data not shown). Because the leaf phenotype was the most striking feature, we focused on this organ.

In the T2 population, the leaf phenotype segregated strictly with the presence and expression of the transgene. The number of leaves was unchanged (per wild-type plant, the mean was 7.25 ± 0.85 [n = 139] compared with 7.28 ± 1.06 [n = 137] and 7.54 ± 1.03 [n = 196] in two independent

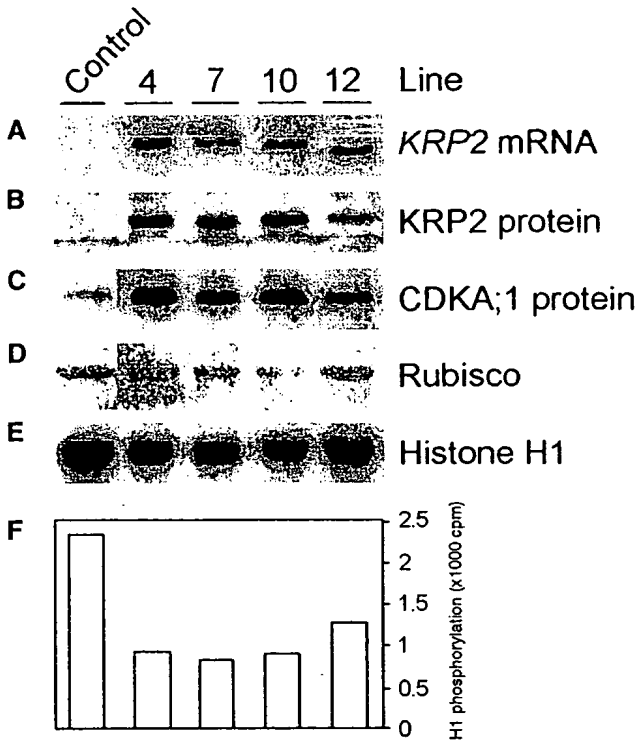

Figure 5. *KRP2* Transgene Expression and CDK Histone H1 Activity in Untransformed and Four Independent Transgenic Arabidopsis Plants.

(A) *KRP2* mRNA levels.
(B) KRP2 protein levels.
(C) CDKA;1 protein levels.
(D) Ribulose-1,5-bisphosphate carboxylase/oxygenase (Rubisco) protein levels visualized by Ponceau S staining (loading control).
(E) CDK histone H1 activity bound to $p10^{CKS1At}$ beads.
(F) Quantification of signals in **(E)**.

KRP2 transgenic plants). Microscopic analysis of mature fifth leaves revealed that all tissue layers in leaves of the KRP2-overproducing lines had much larger cells than did those of control plants, as illustrated for the adaxial epidermis (Figures 6E and 6F) and palisade parenchyma (Figures 6G and 6H). For the adaxial epidermis, the mean cell area was increased almost sixfold, from 599 ± 155 μm^2 in the wild-type plants to 3334 ± 1538 μm^2 in the transgenic plants. Palisade cell area was threefold larger (from 357 ± 31 to 1210 ± 572 μm^2). Similarly, larger cells were observed in the spongy parenchyma and the abaxial epidermis. No difference in cell size was observed for stomata and trichomes, although occasionally enlarged stomata were seen in the cotyledons (data not shown). Transverse sections through the central part of the first leaf revealed that, in addition to having larger areas, all cell types were enlarged conspicuously in the dorsoventral direction (Figure 7). The number of cell layers, however, was unaffected by the transgene, and consequently, KRP2 leaves were somewhat thicker than wild-type leaves (112.48 ± 18.56 μm in KRP2-overproducing lines compared with 89.23 ± 27.17 μm [n = 4] in wild-type plants).

To gain insight into the effect of *KRP2* overexpression on leaf development and cell cycle duration, a kinematic analysis was performed on the first two initiated leaves of plants grown in vitro. We measured cell size and stomatal index on positions 25 and 75% from the base to the tip of the leaf, which, in addition to giving better estimates for the average of the leaf, also allowed detection of the presence of developmental gradients along the length of the blade. The average of the cell areas in these two positions was used in combination with the measured total leaf area to estimate total cell number per leaf. To validate this approach, we took a number of 9-day-old leaves of both wild-type and KRP2-overproducing plants that showed strong basipetal developmental gradients in cell size and stomatal complexes, indicating that they were approximately at the end of their meristematic development. The entire abaxial epidermis of these leaves was drawn on paper with the aid of a drawing tube. On these images, we manually counted the number of epidermal cells and subsequently estimated this number by extrapolating the average cell size at the two reference positions to the whole leaf area. This comparison showed no significant difference between estimated and counted numbers for either genotype (the estimates were 7 ± 4% and 1 ± 10% [average ± SE; n = 5 and 3] higher than the actual counts for ecotype Columbia and KRP2-overproducing plants, respectively).

We used leaves 1 and 2 because they are nearly indistinguishable and probably are best synchronized among replicate plants. From day 5 until day 21 after sowing, leaves of transgenic and wild-type plants were harvested and leaf size and number, size of the abaxial epidermal cells, and stomatal index were determined (see Methods). As can be seen from the linear increase on the logarithmic plot, the leaf area expanded exponentially until day 11 in both wild-type and transgenic lines, after which expansion rates decreased; the mature size was reached approximately 3 weeks after sowing (Figure 8A). Clearly, the duration of expansion was unaffected by the transgene. At maturity, the areas of leaves of the transgenic line were only 25% of those of wild-type leaves (4 and 16 mm^2, respectively). At day 5, however, the primordia of the transgenic lines were, if anything, slightly larger than those of wild-type lines. Thus, the differences in mature leaf size were caused entirely by differences in leaf expansion rates.

The number of abaxial epidermal cells in mature leaves also increased exponentially (Figure 8B). In mature leaves of KRP2-overproducing plants, 10-fold fewer cells were present than in wild-type leaves, whereas at day 5 the cell number differed only slightly. Average cell division rates for the whole leaf could be calculated as exponential increase of the cell number (Figure 8C). Analogous to expansion of

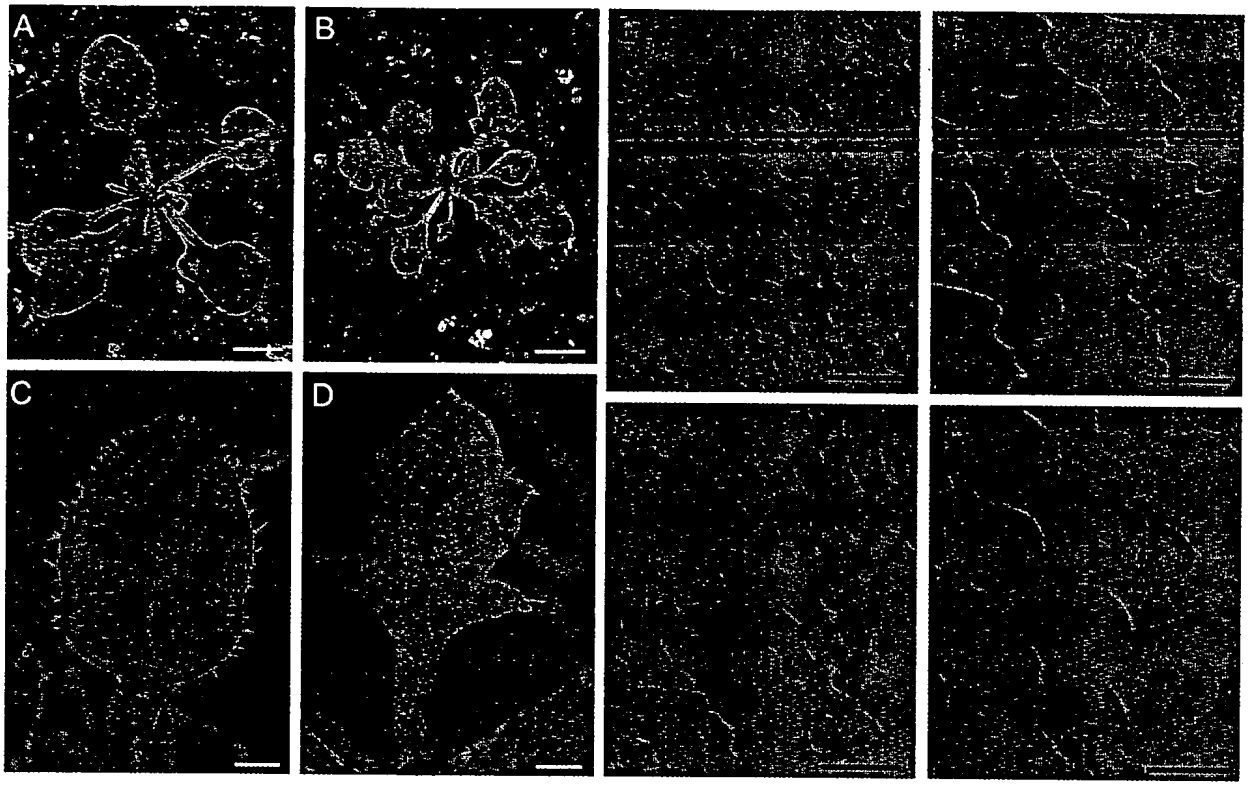

Figure 6. Phenotypic Analysis of KRP2-Overproducing Lines.

(A) Four-week-old soil-grown control plant. The inflorescence was removed to visualize the rosette leaves.
(B) KRP2-overproducing plant with removed inflorescence.
(C) Fifth leaf of a control plant grown in vitro.
(D) Fifth leaf of a KRP2-overproducing plant.
(E) Adaxial epidermal cells of the fifth leaf of a control plant.
(F) Adaxial epidermal cells of a KRP2-overproducing plant.
(G) Palisade cells of the fifth leaf of a control plant.
(H) Palisade cells of a KRP2-overproducing plant.
Bars in **(A)** and **(B)** = 2 mm; bars in **(C)** and **(D)** = 5 mm; bars in **(E)** to **(H)** = 50 μm.

the leaf, the period in which cell division occurred was not influenced by *KRP2* overexpression; cell division rates were approximately constant until 9 days after sowing, then they decreased rapidly during the next 4 to 5 days in both control and transgenic lines. Average cell cycle duration, the time between one phase of mitosis and the next, can be estimated as the inverse of cell division rate. Between days 5 and 9, the average cell cycle duration more than doubled from 20.7 hr in wild-type plants to 43.3 hr in KRP2-overproducing lines.

Average cell size depends on the balance between division and expansion rates (Green, 1976). In the control line, the average cell size was approximately constant during the entire period of cell division, from day 5 to day 9 (Figure 8D), indicating that cell division and expansion rates were balanced. After day 9, cell size increased exponentially because expansion continued in the absence of division. In contrast, in the KRP2-overproducing lines, the average cell size had already increased during the period of cell division, indicating that division rates were more inhibited than were expansion rates. From the start of the analysis at day 5, there was a large difference in cell size between the transgenic and control lines, which must originate from a developmental stage before those studied here.

In Arabidopsis, exit from cell division followed by cell enlargement and differentiation starts at the tip of the leaf and progresses subsequently in a basipetal direction (Pyke et al., 1991). To verify the validity of average cell division rates for the whole leaf and to analyze the effects of *KRP2* overexpression on developmental timing, we determined the evolution of the stomatal index. Divisions that give rise to stomata are the final divisions that occur at a particular position (Donnelly et al., 1999), indicating the end of proliferative activity. The stomatal index was measured in both the

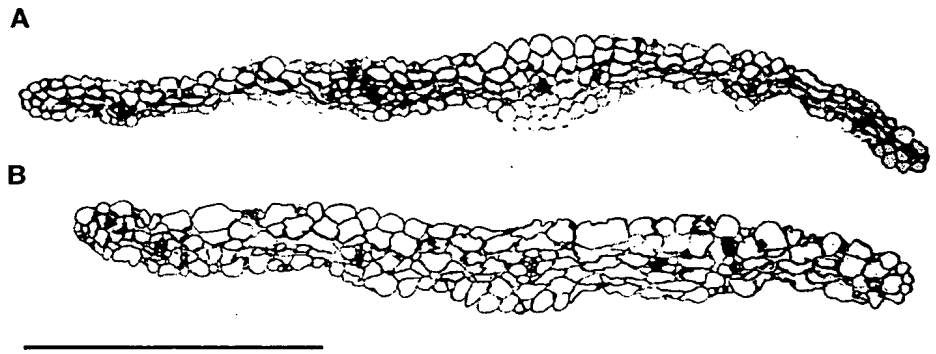

Figure 7. Transverse Sections through the Central Part of the First Leaf.

(A) Sixteen-day-old wild-type leaf grown in vitro.
(B) Sixteen-day-old KRP2-overproducing leaf grown in vitro.
Bar = 500 μm.

tip and the base of the leaves (Figure 8E). The stomatal index remained close to zero until day 9 and then increased until ~15 days after sowing. Stomata were first observed at the tip of the leaf, and the final index was reached a few days earlier, reflecting the basipetal direction of maturation. These data indicate that some cells started leaving the cell cycle 9 days after sowing and that cell division finally stopped at approximately day 15, corresponding well with the independently determined cell division data. The final stomatal index and its evolution were very similar in wild-type and transgenic lines, showing that KRP2 did not influence the timing or the degree of cell differentiation.

KRP2 Overproduction Suppresses Endoreduplication

Arabidopsis leaves undergo extensive endoreduplication, increase of DNA content by consecutive doubling of the genomic DNA in the absence of chromatin segregation, and cytokinesis. A positive correlation between DNA level and cell size has been established (Melaragno et al., 1993; Folkers et al., 1997). Because *KRP2* overexpression results in enlarged cells, the ploidy levels of both wild-type and KRP2-overproducing lines were measured. Different seed stocks often germinate at different times, resulting in small differences in ploidy levels at the moment of analysis. To avoid this problem, we used heterozygous seed stocks of KRP2-overproducing lines. These seed stocks segregated for plants showing normal leaves (1:4) and the serrated leaf phenotype (3:4). Plants were considered as control or transgenic on the basis of their phenotypes. Ploidy levels were analyzed in three different leaves of 3-week-old plants, namely, the youngest leaf (leaf 5), the third leaf, and the oldest leaf (leaf 1). At that stage of development, the youngest leaf is still actively dividing, as seen by the presence of high CDK activity (data not shown), leaf 3 has stopped dividing and is expanding, and leaf 1 is fully expanded and differentiated (Figure 9).

For the youngest leaf, no significant difference between the control and transgenic lines was observed. In wild-type leaves, the fraction of cells with a DNA content of 4C and 8C increased with leaf age at the cost of the 2C fraction because of endoreduplication (Figure 9). This result is in agreement with earlier reports (Galbraith et al., 1991; Jacqmard et al., 1999) demonstrating that the process of endoreduplication is regulated developmentally. In *KRP2*-overexpressing plants, this decrease was significantly slower, showing that, in addition to proliferation, *KRP2* overexpression inhibits the endoreduplication cycle. It can be concluded that the observed cell enlargement occurred in the absence of enhanced endoreduplication.

DISCUSSION

By means of two-hybrid screening and database mining, we identified seven different genes from Arabidopsis with sequence identity to the mammalian CKI $p21^{Kip1}$. Sequence similarity is restricted to a region of ~25 amino acids located at the extreme C-terminal end of each KRP protein. The remaining parts of the KRPs are not significantly similar to those of any protein in the databases. The CDK inhibitory and binding domains of $p27^{Kip1}$ consist of three structural domains: a β-hairpin, a β-strand, and a 3_{10} helix (Russo et al., 1996). The first two structures associate with the N-terminal lobe of the CDKs, resulting in the destabilization of the ATP binding site. The 3_{10} helix binds to the catalytic cleft and occupies the ATP binding site. The KRPs share only sequence identity along the β-hairpin and β-strand and lack the 3_{10} helix. Nevertheless, CDK activity is inhibited by at least

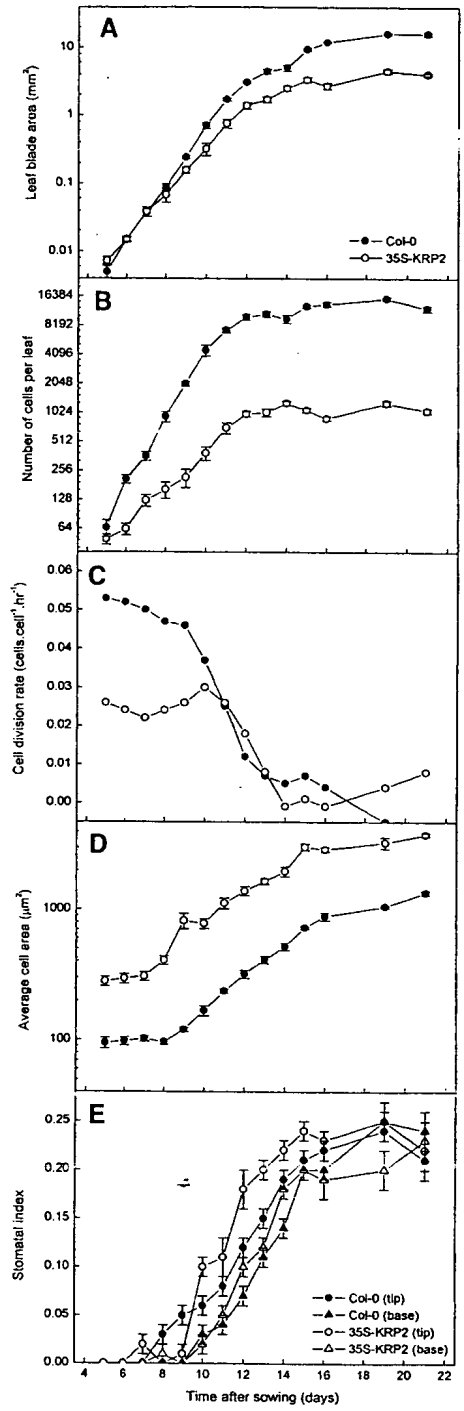

Figure 8. Kinematic Analysis of Leaf Growth of the First Leaf Pair of Wild-Type (Col-0) and KRP2-Overproducing (35S-KRP2) Plants.

(A) Leaf blade area.

(B) Epidermal cell number on the abaxial side of the leaf.

(C) Average cell division rates of the epidermal cells on the abaxial side of the leaf.

(D) Epidermal cell size on the abaxial side of the leaf.

(E) Stomatal index on the abaxial side of the leaf.

Error bars denote standard errors (n = 4 to 10). Symbols in **(B)**, **(C)**, and **(D)** as in **(A)**.

some of the KRPs in vitro (KRP1 and KRP2; Wang et al., 1997; Lui et al., 2000), in a yeast assay (KRP1, KRP2, and KRP4; this study), and in planta (KRP1, KRP2, and KRP3; Wang et al., 2000; this study), showing that the 3_{10} helix domain is not required for CDK inhibition. This result is consistent with the observation that a truncated form of $p27^{Kip1}$ that lacks the 3_{10} helix still retains inhibitory activity (Polyak et al., 1994; Luo et al., 1995).

Why has Arabidopsis so many CKIs? One reason might be related to the diversity of spatial patterns of transcript accumulation, suggesting that KRPs could operate in a tissue-specific manner. Furthermore, differences in the domain organization suggest that the distinct KRPs have dissimilar biochemical properties. We identified distinct sequence motifs within the KRPs, of which only three are shared by all family members. Although the major CDK and cyclin binding domain of the KRPs have been mapped at the C-terminal domain (Wang et al., 1998), the additional motifs found in the N-terminal part of the KRPs could help to determine specificity toward different cyclin/CDK complexes. Alternately, these domains might interact with other unknown proteins. Kip/Cip family members are reported to interact with many other regulatory proteins, including the proliferating cell nuclear antigen (Chen et al., 1995), the coactivator of c-Jun JAB1 (Tomoda et al., 1999), and the syntaxin-like molecule CARB (McShea et al., 2000).

In addition to the different motifs found in the KRPs, they also can be distinguished by the presence (KRP2, KRP4, KRP5, and KRP7) or absence (KRP1, KRP3, and KRP6) of a nuclear localization signal, the presence (KRP2, KRP5, and KRP6) or absence (KRP1, KRP3, KRP4, and KRP7) of PEST domains, and the presence (KRP6 and KRP7) or absence (KRP1, KRP2, KRP3, KRP4, and KRP5) of a consensus CDK phosphorylation site. A CDK phosphorylation site also has been identified in $p27^{Kip1}$. Phosphorylation triggers the degradation of $p27^{Kip1}$ by the ubiquitin/proteasome-dependent pathway, allowing cells to enter the S phase (Vlach et al., 1997; Tomoda et al., 1999). Ubiquitin-dependent degradation of cell cycle proteins in plants has been reported previously (Genschik et al., 1998). In addition, a ubiquitin-ligase complex has been isolated from Arabidopsis (Gray et al., 1999), opening the possibility that the phosphorylation of KRP6 and KRP7 triggers their own destruction in a manner similar to that reported for $p27^{Kip1}$.

The overexpression of *KRP2* affected various organs differentially, the most obvious effect being a large reduction in leaf area. The ~75% reduction in leaf area (Figure 8) was offset by an ~30% increase in leaf thickness (Figure 7).

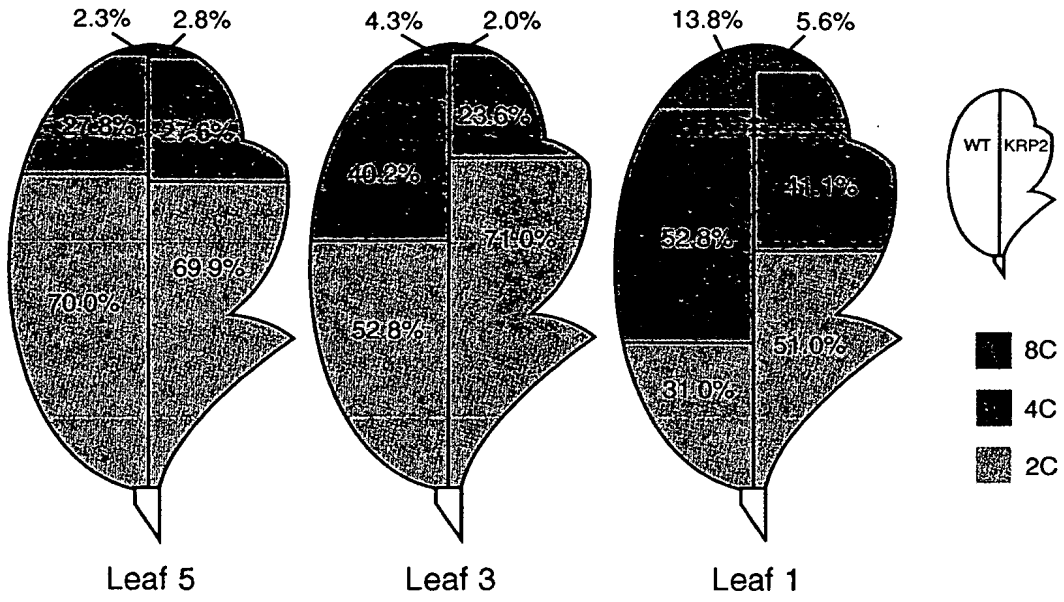

Figure 9. Ploidy Distribution Diagrams of Leaves of Wild-Type (WT) and *KRP2*-Overexpressing Lines.

Values are means of two independent measurements. Maximum differences found between two samples were 4.0, 3.0, and 2.0% for 2C, 4C, and 8C, respectively.

Hence, leaf volume was reduced by approximately two-thirds in response to the transgene. The inhibitory effect on leaf area expansion was studied in detail for the KRP2-overproducing lines with a kinematic approach. This method, which has been used previously for dicotyledonous leaves (Granier and Tardieu, 1998), was adapted to the small size of Arabidopsis leaves. With this method, we found almost constant division rates in epidermal cells during the first 9 days after sowing, after which division stopped rapidly, a pattern similar to that observed in sunflower (Granier and Tardieu, 1998). Moreover, the average cell cycle duration of approximately 20 hr corresponds very well with that found in Arabidopsis root tip meristems growing under similar conditions (Beemster and Baskin, 1998).

In the KRP2-overproducing lines, a decrease of 50 to 60% in CDK activity was measured. Because CDK activity was shown to correlate linearly with growth rates (Granier et al., 2000), KRP2-overproducing plants were expected to grow twice as slowly as controls, which is exactly what we observed: an increase of the cell cycle duration from 20 to 43.3 hr. Whereas the timing of the duration of division and expansion during development remained unaltered, mature leaves showed a more than 10-fold reduced epidermal cell number compared with wild-type plants. Because the number of cell layers did not vary (Figure 7), these data suggest that KRP2 primarily regulates the rate and, thereby, the total number of anticlinal cell divisions during leaf development. Surprisingly, *KRP2* overexpression did not alter the period in which cell division occurred, nor did it influence the timing of cell differentiation, which was measured by the appearance of stomata, suggesting that KRP2, unlike its mammalian counterpart $p27^{Kip1}$, does not regulate cell cycle exit and the onset of cell differentiation. Some of the other KRPs might be involved in these processes.

In the young leaves, no significant differences in ploidy levels were observed between the control and transgenic lines, indicating that both the G1-to-S and G2-to-M transitions are inhibited by KRP2. This conclusion is in agreement with the observation that KRP2 specifically binds CDKA;1, which displays kinase activity at both transition points. In the KRP2 transgenic plants, progression from 2C to 8C was slower than in wild-type plants. Apparently, not only the mitotic cell cycle but the endoreduplication cycle as well is delayed by KRP2 overproduction.

Previously, a correlation was observed between ploidy level and cell size in wild-type epidermal cells and trichomes, suggesting that endoreduplication levels could determine cell size (Melaragno et al., 1993; Folkers et al., 1997). In contrast to these results, our data on KRP2-overproducing lines showed that the leaves displayed enlarged cells, whereas DNA replication clearly was suppressed, illustrating that DNA amplification is not a prerequisite for cell enlargement.

In the KRP2-overproducing lines, an increase in cell size compensated partially for the cell division inhibition, reflecting an uncoupling of cell growth from cell division. A similar uncoupling, which has been seen in tobacco plants with reduced A-type CDK activity (Hemerly et al., 1995), illustrates the plasticity of cells in response to changes in cell division ac-

tivity. In contrast to this uncoupling of division and expansion, leaf morphology was changed: in the KRP2-overproducing lines, the slightly serrated phenotype that can be observed in control plants became very pronounced. In analogy to the differential sensitivity between organs, the inhibitory effect of KRP2 in specific domains of the leaf might underlie this phenotype. It has been noted that the expression of *CYCB1;1* and *CYCA2;1* at the leaf teeth remains high during late foliar development, when these mitotic cyclins are already not expressed in other parts of the leaves (Van Lijsebettens and Clarke, 1998; Burssens et al., 2000). Therefore, increased KRP2 levels might be less effective at inhibiting cell division activity at the teeth. However, to understand exactly how *KRP2* overexpression results in abnormal leaf morphology, it will be necessary to determine when differences in shape become apparent during leaf development and how this is correlated with changes in cell division rates.

KRP2 is not the only cell cycle gene that induces abnormal leaf morphology. Overexpression of the fission yeast *cdc25* gene in tobacco results in plants in which the leaves show a twisted appearance, with the interveinal regions being pocketed (Bell et al., 1993). Because overexpression of *cdc25* is supposed to stimulate CDK activity positively, this phenotype may be the opposite of the KRP2-induced phenotype. No change in leaf morphology was reported upon the overproduction of other core cell cycle proteins, such as CDKA;1, CYCD2;1, CYCB1;1, and CKS1At (Hemerly et al., 1995; Doerner et al., 1996; Cockcroft et al., 2000; De Veylder et al., 2001). Because the serrated leaf phenotype also was observed in plants that overexpressed *KRP1* or *KRP3*, it remains unknown whether KRP2 has a true morphogenic function or whether the observed phenotype is secondary to the strong reduction in cell number. Regardless, our data show that the rate of cell division can be an important factor in determining leaf shape.

METHODS

Isolation of Kip-Related Protein Genes

A two-hybrid screen using the CDKA;1 protein as a bait was performed as described (De Veylder et al., 1999). Among the positive clones, three different $p27^{Kip1}$-like genes were identified: *KRP1*, *KRP2*, and *KRP3*. Full-length clones were obtained by screening a flower cDNA library obtained from the Arabidopsis Biological Resources Center (library number CD4-6; Columbus, OH). By screening the Arabidopsis databases, four additional *KRP* genes were discovered located on the genomic clones with accession numbers AC003974 (*KRP4*), AB028609 (*KRP5*), AP000419 (*KRP6*), and AC011807 (*KRP7*). The corresponding cDNAs were isolated using RNA prepared from cell suspensions of *Arabidopsis thaliana* (ecotype Columbia [Col-0]) and the Superscript RT II kit (Gibco BRL, Gaithersburg, MD) according to the manufacturer's protocol. Primers used were 5′-CCGGAATTCATGGGGAAATACATAAGAAAGAGC-3′ and 5′-GGCGGATCCGTTTCTAATCATCTACCTTCGTCC-3′ for *KRP4*, 5′-GGGAATTCATGGGAAAATACATTAAG-3′ and 5′-GGGGATCCTCATGGCATCACTTTGACC-3′ for *KRP5*, 5′-GGGAATTCATGAGCGAGAGAAAGCG-3′ and 5′-GGGGATCCTTAAAGTCGATCCC-3′ for *KRP6*, and 5′-GGGAATTCATGAGCGAAACAAAACCC-3′ and 5′-GGGGATCCCTAAGGTTTCAGACTAACCC-3′ for *KRP7*. The resulting polymerase chain reaction (PCR) fragments were cut with EcoRI and BamHI and cloned into the EcoRI and BamHI sites of pGBT9 and pGAD424 (Clontech, Palo Alto, CA), resulting in the vectors pGADKRP4, pGADKRP5, pGADKRP6, pGADKRP7, pGBTKRP4, pGBTKRP5, pGBTKRP6, and pGBTKRP7. Binding specificity of the different Kip-related proteins (KRPs) toward CDKA;1, CDKB1;1, and CYCD4 was tested as described (De Veylder et al., 1997). Motifs were identified using the GCG software package (Genetics Computer Group, Madison, WI).

Reverse Transcriptase–Mediated PCR Analysis

RNA was isolated from flowers, roots, inflorescence stems, and 3-day-old cell suspensions of Arabidopsis (ecotype Col-0) using Trizol reagent (Amersham Pharmacia Biotech, Little Chalfont, UK). The RNA was treated with DNase for 30 min and was column purified (Chromaspin 400; Clontech). First-strand cDNA synthesis was performed on 3 μg of total RNA with the Superscript RT II kit (Gibco BRL) and oligo$(dT)_{18}$ according to the manufacturer's instructions. A 1-μL aliquot of the total reverse transcription reaction volume (20 μL) was used as a template in semiquantitative reverse transcriptase–mediated PCR amplification, ensuring that the amount of amplified product remained in linear proportion to the initial template present in the reaction. Ten microliters from the PCR reaction was separated on a 0.8% agarose gel and transferred onto Hybond N^+ membranes (Amersham Pharmacia Biotech). The membranes were hybridized at 65°C with fluorescein-labeled probes (Gene Images random prime module; Amersham Pharmacia Biotech). The hybridized bands were detected using the CDP Star detection module (Amersham Pharmacia Biotech). Primers used were 5′-GCAGCTACGGAGCCGGAGAATTGT-3′ and 5′-TCTCCTTCTCGAAATCGAAATTGTACT-3′ for *KRP1*, 5′-CGGCTCGAGGAGAACCACAAACACGC-3′ and 5′-CGAAACTAGTTAATTACCTCAAGGAAG-3′ for *KRP2*, 5′-GATCCCGGGCGATATCAGCGTCATGG-3′ and 5′-GATCCCGGGTTAGTCTGTTAACTCC-3′ for *KRP3*, 5′-GGCGGATCCGTTTCTAATCATCTACCTTCGTCC-3′ and 5′-GAATCCATGGGGTACATAAG-3′ for *KRP4*, 5′-GGCCATGGGAAAATACATTAAGAA-3′ and 5′-GGGGATCCTCATGGCATCACTTTGACC-3′ for *KRP5*, 5′-GGCCATGGGCGAGAGAAAGCGAGAGC-3′ and 5′-GGGGATCCTTAAAGTCGATCCC-3′ for *KRP6*, 5′-GGCCATGGGCGAAACAAAACCCAAGAG-3′ and 5′-GGGGATCCCTAAGGTTTCAGACTAACCC-3′ for *KRP7*, and 5′-CTAAGCTCTCAAGATCAAAGGCTTA-3′ and 5′-TTAACATTGCAAAGAGTTTCAAGGT-3′ for *ACT2*.

Generation of KRP2 and KRP3 Proteins and Antibodies

The coding regions of *KRP2* and *KRP3* were amplified by PCR. The KRP3-amplified coding sequence contained a protein starting at Met-11. Primer pairs used to amplify *KRP2* and *KRP3* were 5′-TAGGAGCATATGGCGGCGG-3′ and 5′-ATCATCGAATTCTTCATGGATTC-3′ and 5′-ATATCAGCGCCATGGAAGTC-3′ and 5′-GGAGCTGGATCCTTTTGGAATTCATGG-3′, respectively. The obtained *KRP2* PCR fragment was cut with NdeI and EcoRI and cloned into the NdeI

and EcoRI sites of pRK172 (McLeod et al., 1987). The obtained *KRP3* PCR fragment was cut with NcoI and BamHI and cloned into the NcoI and BamHI sites of pET21d. KRP3pET21d was transformed into *Escherichia coli* BL21(DE3). KRP2pRK172 was cotransformed into *E. coli* BL21(DE3) with pSBETa (Schenk et al., 1995). pSBETa encoded $tRNA^{UCU}$, which is a low-abundance tRNA in *E. coli* corresponding to codons AGG and AGA (Arg). Because of the presence of an AGGAGAAGA sequence (Arg-5, Arg-6, and Arg-7) at the beginning of the *KRP2* coding sequence, an increase of the $tRNA^{UCU}$ pool of *E. coli* was necessary for the translation of *KRP2*.

The KRP3pET21d/BL21(DE3) and KRP2pRK172[pSBETa/BL21(DE3)] *E. coli* recombinant strains were grown on selective Luria-Bertani medium. The cells were grown at 37°C until the density of the culture reached A_{600} = 0.7. At this time, 0.4 mM isopropyl-β-D-thiogalactopyranoside was added to induce production of the recombinant protein. Cells were collected 3 hr later by centrifugation. The bacterial pellet from 250 mL of culture was suspended in 10 mL of lysis buffer (Tris-HCl, pH 7.5, 1 mM DTT, 1 mM EDTA, 1 mM phenylmethylsulfonyl fluoride, and 0.1% Triton X-100) and subjected to three freeze/thaw cycles before sonication. Cell lysate was clarified by centrifugation for 20 min at 8000 rpm. The pellet was collected and resuspended in extraction buffer. Third and fourth washes were performed in the same way with Tris extraction buffer with and without 1 M NaCl, respectively.

After the different washing steps, the pellet contained KRP3 or KRP2 proteins at 90% homogeneity. The pellets were suspended in Laemmli loading buffer (Laemmli, 1970), and KRP3 and KRP2 were further purified by SDS-12% PAGE. The gel was stained in 0.025% Coomassie Brilliant Blue R 250 in water and destained in water. The strong band comigrating at the 31-kD marker position was cut from the gel with a scalpel. The polyacrylamide fragments containing KRP3 or KRP2 were lyophilized and reduced to powder. The rabbit immunization was performed subcutaneously with complete Freund's adjuvant with this antigen preparation. One injection corresponded to 100 μg of protein. The boosting injections were performed subcutaneously with incomplete Freund's adjuvant. With the obtained sera, bands of the expected size were found in protein extracts prepared from 2-day-old actively dividing cell cultures. No signals were observed with the preimmune serum.

In Vitro KRP3 Binding Assay

Purified recombinant KRP3 protein was coupled to cyanogen bromide–activated Sepharose 4B (Amersham Pharmacia Biotech) at a concentration of 5 mg/mL according to the manufacturer's instructions. Protein extracts were prepared from a 2-day-old cell suspension culture of Arabidopsis Col-0 in homogenization buffer (HB) containing 50 mM Tris-HCl, pH 7.2, 60 mM β-glycerophosphate, 15 mM nitrophenyl phosphate, 15 mM EGTA, 15 mM $MgCl_2$, 2 mM DTT, 0.1 mM vanadate, 50 mM NaF, 20 μg/mL leupeptin, 20 μg/mL aprotinin, 20 μg/mL soybean trypsin inhibitor, 100 μM benzamidine, 1 mM phenylmethylsulfonyl fluoride, and 0.1% Triton X-100. Protein extract (200 μg) in a total volume of 100 μL of HB was loaded onto 50 μL of 50% (v/v) KRP3-Sepharose or control Sepharose beads and incubated on a rotating wheel for 2 hr at 4°C. The unbound proteins were collected for later analysis. The bead-bound fractions were washed three times with HB. The beads were resuspended in 30 μL of SDS loading buffer and boiled. The supernatants (bead-bound fractions) and 10 μL of the unbound fractions were separated on a 12.5% SDS-polyacrylamide gel and electroblotted onto nitrocellulose membranes (Hybond C+; Amersham Pharmacia Biotech). Filters were blocked overnight with 2% milk in PBS, washed three times with PBS, probed for 2 hr with specific antibodies for CDKA;1 (1:5000 dilution) or CDKB1;1 (1:2500 dilution) in PBS containing 0.5% Tween 20 and 1% albumin, washed for 1 hr with PBS containing 0.5% Tween 20, incubated for 2 hr with peroxidase-conjugated secondary antibody (Amersham Pharmacia Biotech), and washed for 1 hr with PBS containing 0.5% Tween 20. Proteins were detected by the chemiluminescence procedure (Pierce Chemical Co., Rockford, IL).

Regeneration and Molecular Analysis of *KRP2*-Overexpressing Plants

The full length KRP2 coding region was amplified by PCR with the 5′-AGACCATGGCGGCGGTTAGGAG-3′ and 5′-GGCGGATCC-CGTCTTCTTCATGGATTC-3′ primers, introducing NcoI and BamHI restriction sites. The amplified fragment was cut with NcoI and BamHI and cloned between the NcoI and BamHI sites of PH35S (Hemerly et al., 1995), resulting in the 35SKRP2 vector. The cauliflower mosaic virus 35S/KRP2/nopaline synthase cassette was released by EcoRI and XbaI and cloned blunt into the SmaI site of PGSV4 (Hérouart et al., 1994). The resulting vector, PGSKRP2, was mobilized by the helper plasmid pRK2013 into *Agrobacterium tumefaciens* C58C1Rif^R harboring the plasmid pMP90. Arabidopsis plants (ecotype Col-0) were transformed by the floral dip method (Clough and Bent, 1998). Transgenic plants were obtained on kanamycin-containing medium and later transferred to soil for optimal seed production. For all analyses, plants were grown in vitro under a 16-hr-light/8-hr-dark photoperiod at 22°C on germination medium (Valvekens et al., 1988). Molecular analysis of the obtained transformants was performed by RNA and protein gel blotting, and cyclin-dependent kinase (CDK) activity measurements were as described (De Veylder et al., 1997, 1999). Leaves were sectioned according to Beeckman and Viane (2000).

Kinematic Analysis of Leaf Growth

For the kinematic analysis of leaf growth, eight plants of the wild type and three KRP2-overproducing lines were sown in quarter sections of round 12-cm Petri dishes filled with 100 mL of 1 × Murashige and Skoog (1962) medium (Duchefa, Haarlem, The Netherlands) and 0.6% plant tissue culture agar (Lab M, Bury, UK). The plates were placed horizontally on cooled benches in a growth chamber (temperature, 22°C; irradiation, 65 $\mu E \cdot m^{-2} \cdot sec^{-1}$ photosynthetically active radiation; photoperiod, 16-hr-light/8-hr-dark). From day 5 (when cotyledons started to expand) until day 21 after sowing (when leaves were fully expanded), a single plate was harvested daily (except on days 17, 18, and 20). All healthy plants were placed in methanol overnight to remove chlorophyll, and subsequently they were cleared and stored in lactic acid for microscopy.

A strong *KRP2*-overexpressing line was selected for analysis. The youngest plants were mounted whole on a slide and covered. Older primordia that had visible petioles were dissected, whereas younger primordia were left on the plant. The primordia were observed with differential interference contrast optics on a microscope (DMLB; Leica, Wetzlar, Germany). The total leaf (blade) area of the oldest two primordia (leaves 1 and 2) of each seedling was determined from

drawing tube images that were scanned with a flatbed scanner using the public domain image analysis program ImageJ (version 1.17y; http://rsb.info.nih.gov/ij/). At older stages, the primordia were digitized directly with a charge-coupled device camera mounted on a binocular (Stemi SV11; Zeiss, Jena, Germany), which was connected to a personal computer fitted with a frame-grabber board LG3 (Scion Corp., Frederick, MD) running the image analysis program Scion Image (version 3b for Windows NT).

Cell density and stomatal index were determined from scanned drawing tube images of outlines of at least 20 cells of the abaxial epidermis located 25 and 75% from the distance between the tip and the base of the leaf primordium (or blade once the petiole was present), halfway between the midrib and the leaf margin. In the youngest primordia (up to day 6), a single group of cells was drawn. The following parameters were determined: total area of all cells in the drawing, total number of cells, and number of guard cells. From these data, we calculated the average cell area and the stomatal index (i.e., the fraction of guard cells in the total population of epidermal cells). We estimated the total number of cells per leaf by dividing the leaf area by the average cell area (averaged between the apical and basal positions). Finally, average cell division rates for the whole leaf were determined as the slope of the log 2–transformed number of cells per leaf, which was done using five-point differentiation formulas (Erickson, 1976).

Flow Cytometric Analysis of Leaves

Leaves were chopped with a razor blade in 300 μL of buffer (45 mM $MgCl_2$, 30 mM sodium citrate, 20 mM 3-[*N*-morpholino]propanesulfonic acid, pH 7, and 1% Triton X-100) (Galbraith et al., 1991). To the supernatants, 1 μL of 4′,6-diamidino-2-phenylindole from a stock of 1 mg/mL was added, which was filtered over a 30-μm mesh. The nuclei were analyzed with the BRYTE HS flow cytometer and WinBryte software (Bio-Rad, Hercules, CA).

KRP2 Analysis in Yeast

The *CDKA;1.A14F15* and *KRP2* genes were fused transcriptionally to the *nmt1* promoter in the fission yeast vectors pREP41 (with a leucine marker) and pREP4X (with a uracil marker), respectively (Maundrell, 1993). The pREPCDKA;1.A14F15 vector has been described (Porceddu et al., 1999). The pREP4KRP2 vector was obtained by cloning the *KRP2* gene into the XhoI and BamHI sites of the pREP4X vector after the XhoI and BamHI sites had been introduced by PCR with the primers 5′-GGCATATGGCGGCGGTTAGGAG-3′ and 5′-GGCGGATCCCGTCTTCTTCATCATGGATTC-3′. Plasmids were transformed into the fission yeast strain *972 leu1-32 ura4-D18 h*$^-$ using the lithium acetate method (Gietz et al., 1992). All yeast manipulations were performed as described (Porceddu et al., 1999).

GenBank Accession Numbers

The GenBank accession numbers are as follows: KRP1, U94772; KRP2, AJ251851; KRP3, AJ301554; KRP4, AJ301555; KRP5, AJ301556; KRP6, AJ301557; KRP7, AJ301558; Chenopodium KRP, AJ002173.

ACKNOWLEDGMENTS

The authors thank the members of the cell cycle group for fruitful discussions and useful suggestions. Stefaan Rombauts for analyzing the sequences, Martine De Cock for help in preparing the manuscript, and Peter Chaerle, Rebecca Verbank, Stijn Debruyne, and Karel Spruyt for illustrations. This work was supported by grants from the Interuniversity Poles of Attraction Program (Belgian State, Prime Minister's Office, Federal Office for Scientific, Technical and Cultural Affairs; P4/15) and the European Union (ECCO QLG2-CT1999-00454). L.D.V. is indebted to the "Onderzoeksfonds van de Universiteit Gent" for a postdoctoral fellowship.

Received March 2, 2001; accepted May 17, 2001.

REFERENCES

Beeckman, T., and Viane, R. (2000). Embedding thin plant specimens for oriented sectioning. Biotech. Histochem. **75,** 23–26.

Beemster, G.T.S., and Baskin, T.I. (1998). Analysis of cell division and elongation underlying the developmental acceleration of root growth in *Arabidopsis thaliana*. Plant Physiol. **116,** 1515–1526.

Bell, M.H., Halford, N.G., Ormrod, J.C., and Francis, D. (1993). Tobacco plants transformed with cdc25, a mitotic inducer gene from fission yeast. Plant Mol. Biol. **23,** 445–451.

Burssens, S., de Almeida Engler, J., Beeckman, T., Richard, C., Shaul, O., Ferreira, P., Van Montagu, M., and Inzé, D. (2000). Developmental expression of the *Arabidopsis thaliana CycA2;1* gene. Planta **211,** 623–631.

Chen, J., Jackson, P.K., Kirschner, M.W., and Dutta, A. (1995). Separate domains of p21 involved in the inhibition of Cdk kinase and PCNA. Nature **374,** 386–388.

Cheng, M., Olivier, P., Diehl, J.A., Fero, M., Roussel, M.F., Roberts, J.M., and Sherr, C.J. (1999). The $p21^{Cip1}$ and $p27^{Kip1}$ CDK 'inhibitors' are essential activators of cyclin D-dependent kinases in murine fibroblasts. EMBO J. **18,** 1571–1583.

Clough, S.J., and Bent, A.F. (1998). Floral dip: A simplified method for *Agrobacterium*-mediated transformation of *Arabidopsis thaliana*. Plant J. **16,** 735–743.

Cockcroft, C.E., den Boer, B.G.W., Healy, J.M.S., and Murray, J.A.H. (2000). Cyclin D control of growth rate in plants. Nature **405,** 575–579.

De Veylder, L., Segers, G., Glab, N., Casteels, P., Van Montagu, M., and Inzé, D. (1997). The Arabidopsis Cks1At protein binds to the cyclin-dependent kinases Cdc2aAt and Cdc2bAt. FEBS Lett. **412,** 446–452.

De Veylder, L., De Almeida Engler, J., Burssens, S., Manevski, A., Lescure, B., Van Montagu, M., Engler, G., and Inzé, D. (1999). A new D-type cyclin of *Arabidopsis thaliana* expressed during lateral root primordia formation. Planta **208,** 453–462.

De Veylder, L., Beemster, G.T.S., Beeckman, T., and Inzé, D. (2001). *CKS1At* overexpression in *Arabidopsis thaliana* inhibits growth by reducing meristem size and inhibiting cell cycle progression. Plant J. **25,** 617–626.

Doerner, P., Jørgensen, J.-E., You, R., Steppuhn, J., and Lamb, C. (1996). Control of root growth and development by cyclin expression. Nature **380,** 520–523.

Donnelly, P.M., Bonetta, D., Tsukaya, H., Dengler, R.E., and Dengler, N.G. (1999). Cell cycling and cell enlargement in developing leaves of *Arabidopsis*. Dev. Biol. **215,** 407–419.

Dulić, V., Kaufmann, W.K., Wilson, S.J., Tlsty, T.D., Lees, E., Harper, J.W., Elledge, S.J., and Reed, S.I. (1994). p53-dependent inhibition of cyclin-dependent kinase activities in human fibroblasts during radiation-induced G1 arrest. Cell **76,** 1013–1023.

Dunphy, W.G. (1994). The decision to enter mitosis. Trends Cell Biol. **4,** 202–207.

Erickson, R.O. (1976). Modeling of plant growth. Annu. Rev. Plant Physiol. **27,** 407–434.

Fero, M.L., Rivkin, M., Tasch, M., Porter, P., Carow, C.E., Firpo, E., Polyak, K., Tsai, L.-H., Broudy, V., Perlmutter, R.M., Kaushansky, K., and Roberts, J.M. (1996). A syndrome of multiorgan hyperplasia with features of gigantism, tumorigenesis, and female sterility in $p27^{Kip1}$-deficient mice. Cell **85,** 733–744.

Folkers, U., Berger, J., and Hülskamp, M. (1997). Cell morphogenesis of trichomes in Arabidopsis: Differential control of primary and secondary branching by branch initiation regulators and cell growth. Development **124,** 3779–3786.

Galbraith, D.W., Harkins, K.R., and Knapp, S. (1991). Systemic endopolyploidy in *Arabidopsis thaliana*. Plant Physiol. **96,** 985–989.

Genschik, P., Criqui, M.C., Parmentier, Y., Derevier, A., and Fleck, J. (1998). Cell cycle–dependent proteolysis in plants: Identification of the destruction box pathway and metaphase arrest produced by the protease inhibitor MG132. Plant Cell **10,** 2063–2075.

Gietz, D., St. Jean, A., Woods, R.A., and Schiestl, R.H. (1992). Improved method for high efficiency transformation of intact yeast cells. Nucleic Acids Res. **20,** 1425.

Granier, C., and Tardieu, F. (1998). Spatial and temporal analyses of expansion and cell cycle in sunflower leaves: A common pattern of development for all zones of a leaf and different leaves of a plant. Plant Physiol. **116,** 991–1001.

Granier, C., Inzé, D., and Tardieu, F. (2000). Spatial distribution of cell division rate can be deduced from that of $p34^{cdc2}$ kinase activity in maize leaves grown at contrasting temperatures and soil water conditions. Plant Physiol. **124,** 1393–1402.

Gray, W.M., del Pozo, J.C., Walker, L., Hobbie, L., Risseeuw, E., Banks, T., Crosby, W.L., Yang, M., Ma, H., and Estelle, M. (1999). Identification of an SCF ubiquitin-ligase complex required for auxin response in *Arabidopsis thaliana*. Genes Dev. **13,** 1678–1691.

Green, P.B. (1976). Growth and cell pattern formation on an axis: Critique of concepts, terminology, and modes of study. Bot. Gaz. **137,** 187–202.

Hemerly, A., de Almeida Engler, J., Bergounioux, C., Van Montagu, M., Engler, G., Inzé, D., and Ferreira, P. (1995). Dominant negative mutants of the Cdc2 kinase uncouple cell division from iterative plant development. EMBO J. **14,** 3925–3936.

Hérouart, D., Van Montagu, M., and Inzé, D. (1994). Developmental and environmental regulation of the *Nicotiana plumbaginifolia* cytosolic Cu/Zn-superoxide dismutase promoter in transgenic tobacco. Plant Physiol. **104,** 873–880.

Jacqmard, A., De Veylder, L., Segers, G., de Almeida Engler, J., Bernier, G., Van Montagu, M., and Inzé, D. (1999). *CKS1At* expression in *Arabidopsis thaliana* suggests a role for the protein in both the mitotic and the endoreduplication cycle. Planta **207,** 496–504.

Joubès, J., Chevalier, C., Dudits, D., Heberle-Bors, E., Inzé, D., Umeda, M., and Renaudin, J.-P. (2000). CDK-related protein kinases in plants. Plant Mol. Biol. **43,** 607–620.

Kato, J.-y., Matsuoka, M., Polyak, K., Massagué, J., and Sherr, C.J. (1994). Cyclic AMP-induced G1 phase arrest mediated by an inhibitor ($p27^{Kip1}$) of cyclin-dependent kinase 4 activation. Cell **79,** 487–496.

LaBaer, J., Garrett, M.D., Stevenson, L.F., Slingerland, J.M., Sandhu, C., Chou, H.S., and Harlow, E. (1997). New functional activities for the p21 family of CDK inhibitors. Genes Dev. **11,** 847–862.

Laemmli, U.K. (1970). Cleavage of structural proteins during the assembly of the head of bacteriophage T4. Nature **227,** 680–685.

Lee, M.-H., Reynisdóttir, I., and Massagué, J. (1995). Cloning of $p57^{KIP2}$, a cyclin-dependent kinase inhibitor with unique domain structure and tissue distribution. Genes Dev. **9,** 639–649.

Lui, H., Wang, H., DeLong, C., Fowke, L.C., Crosby, W.L., and Fobert, P.R. (2000). The Arabidopsis Cdc2a-interacting protein ICK2 is structurally related to ICK1 and is a potent inhibitor of cyclin-dependent kinase activity *in vitro*. Plant J. **21,** 379–385.

Luo, Y., Hurwitz, J., and Massagué, J. (1995). Cell-cycle inhibition by independent CDK and PCNA binding domains in $p21^{Cip1}$. Nature **375,** 159–161.

Magyar, Z., Mészáros, T., Miskolczi, P., Deák, M., Fehér, A., Brown, S., Kondorosi, E., Athanasiadis, A., Pongor, S., Bilgin, M., Bakó, L., Koncz, C., and Dudits, D. (1997). Cell cycle phase specificity of putative cyclin-dependent kinase variants in synchronized alfalfa cells. Plant Cell **9,** 223–235.

Maundrell, K. (1993). Thiamine-repressible expression vectors pREP and pRIP for fission yeast. Gene **123,** 127–130.

McLeod, M., Stein, M., and Beach, D. (1987). The product of the *mei3*$^+$ gene, expressed under control of the mating-type locus, induces meiosis and sporulation in fission yeast. EMBO J. **6,** 729–736.

McShea, A., Samuel, T., Eppel, J.-T., Galloway, D.A., and Funk, J.O. (2000). Identification of CIP-1-associated regulator of cyclin B (CARB), a novel p21-binding protein acting in the G_2 phase of the cell cycle. J. Biol. Chem. **275,** 23181–23186.

Melaragno, J.E., Mehrotra, B., and Coleman, A.W. (1993). Relationship between endopolyploidy and cell size in epidermal tissue of Arabidopsis. Plant Cell **5,** 1661–1668.

Mironov, V., De Veylder, L., Van Montagu, M., and Inzé, D. (1999). Cyclin-dependent kinases and cell division in higher plants: The nexus. Plant Cell **11,** 509–521.

Murashige, T., and Skoog, F. (1962). A revised medium for rapid growth and bioassays with tobacco tissue culture. Physiol. Plant. **15,** 473–497.

Nakayama, K., Ishida, N., Shirane, M., Inomata, A., Inoue, T., Shishido, N., Horii, I., Loh, D.Y., and Nakayama, K.-i. (1996).

Mice lacking $p27^{Kip1}$ display increased body size, multiple organ hyperplasia, retinal dysplasia, and pituitary tumors. Cell **85,** 707–720.

Nourse, J., Firpo, E., Flanagan, W.M., Coats, S., Polyak, K., Lee, M.-H., Massague, J., Crabtree, G.R., and Roberts, J.M. (1994). Interleukin-2-mediated elimination of the $p27^{Kip1}$ cyclin-dependent kinase inhibitor prevented by rapamycin. Nature **372,** 570–573.

Peters, J.-M. (1998). SCF and APC: The yin and yang of cell cycle regulated proteolysis. Curr. Opin. Cell Biol. **10,** 759–768.

Pines, J. (1994). Protein kinases and cell cycle control. Semin. Cell Biol. **5,** 399–408.

Polyak, K., Lee, M.-H., Erdjument-Bromage, H., Koff, A., Roberts, J.M., Tempst, P., and Massagué, J. (1994). Cloning of $p27^{Kip1}$, a cyclin-dependent kinase inhibitor and a potential mediator of extracellular antimitogenic signals. Cell **78,** 59–66.

Porceddu, A., De Veylder, L., Hayles, J., Van Montagu, M., Inzé, D., and Mironov, V. (1999). Mutational analysis of two *Arabidopsis thaliana* cyclin-dependent kinases in fission yeast. FEBS Lett. **446,** 182–188.

Pyke, K.A., Marrison, J.L., and Leech, R.M. (1991). Temporal and spatial development of the cells of the expanding first leaf of *Arabidopsis thaliana* (L.) Heynh. J. Exp. Bot. **42,** 1407–1416.

Rogers, S., Wells, R., and Rechsteiner, M. (1986). Amino acid sequences common to rapidly degraded proteins: The PEST hypothesis. Science **234,** 364–368.

Russo, A.A., Jeffrey, P.D., Patten, A.K., Massagué, J., and Pavletich, N.P. (1996). Crystal structure of the $p27^{Kip1}$ cyclin-dependent-kinase inhibitor bound to the cyclin A–Cdk2 complex. Nature **382,** 325–331.

Schenk, P.M., Baumann, S., Mattes, R., and Steinbiss, H.H. (1995). Improved high-level expression system for eukaryotic genes in *Escherichia coli* using T7 RNA polymerase and rare ArgtRNAs. BioTechniques **19,** 196–200.

Sherr, C.J., and Roberts, J.M. (1995). Inhibitors of mammalian G_1 cyclin-dependent kinases. Genes Dev. **9,** 1149–1163.

Sherr, C.J., and Roberts, J.M. (1999). CDK inhibitors: Positive and negative regulators of G_1-phase progression. Genes Dev. **13,** 1501–1512.

Smith, M.L., Chen, I.-T., Zhan, Q., Bae, I., Chen, C.-Y., Gilmer, T.M., Kastan, M.B., O'Connor, P.M., and Fornace, A.J., Jr. (1994). Interaction of the p53-regulated protein Gadd45 with proliferating cell nuclear antigen. Science **266,** 1376–1380.

Tomoda, K., Kubota, Y., and Kato, J.-y. (1999). Degradation of the cyclin-dependent kinase inhibitor $p27^{Kip1}$ is instigated by Jab1. Nature **398,** 160–165.

Toyoshima, H., and Hunter, T. (1994). p27, a novel inhibitor of G1 cyclin-Cdk protein kinase activity, is related to p21. Cell **78,** 67–74.

Valvekens, D., Van Montagu, M., and Van Lijsebettens, M. (1988). *Agrobacterium tumefaciens*–mediated transformation of *Arabidopsis thaliana* root explants by using kanamycin selection. Proc. Natl. Acad. Sci. USA **85,** 5536–5540.

Van Lijsebettens, M., and Clarke, J. (1998). Leaf development in *Arabidopsis*. Plant Physiol. Biochem. **36,** 47–60.

Vlach, J., Hennecke, S., and Amati, B. (1997). Phosphorylation-dependent degradation of the cyclin-dependent kinase inhibitor $p27^{Kip21}$. EMBO J. **16,** 5334–5344.

Wang, H., Fowke, L.C., and Crosby, W.L. (1997). A plant cyclin–dependent kinase inhibitor gene. Nature **386,** 451–452.

Wang, H., Qi, Q., Schorr, P., Cutler, A.J., Crosby, W.L., and Fowke, L.C. (1998). ICK1, a cyclin–dependent protein kinase inhibitor from *Arabidopsis thaliana* interacts with both Cdc2a and CycD3, and its expression is induced by abscisic acid. Plant J. **15,** 501–510.

Wang, H., Zhou, Y., Gilmer, S., Whitwill, S., and Fowke, L.C. (2000). Expression of the plant cyclin–dependent kinase inhibitor ICK1 affects cell division, plant growth and morphology. Plant J. **24,** 613–623.

Zhang, P., Wong, C., Liu, D., Finegold, M., Harper, J.W., and Elledge, S.J. (1999). $p21^{CIP1}$ and $p57^{KIP2}$ control muscle differentiation at the myogenin step. Genes Dev. **13,** 213–224.